

9

MEAN FLOW/HEAT TRANSFER SIMILARITY
AND
CHARACTER OF FREE STREAM TURBULENCE
IN A HOT TURBINE CASCADE

Prepared by: CENGIZ CAMCI
The Pennsylvania State University
Aerospace Engineering Department

For: SOLAR TURBINES INC. San Diego, CA

17-August-1992

TABLE OF CONTENTS

ABSTRACT

NOMENCLATURE

INTRODUCTION

PRINCIPLES OF MEAN FLOW SIMILARITY FOR A HOT CASCADE RIG

SPECIFIC APPLICATION TO SOLAR HOT CASCADE FACILITY (GAS SIDE)
SPECIFIC APPLICATION TO SOLAR HOT CASCADE FACILITY (COOLANT SIDE)

PAST WORK ON THE CHARACTERIZATION OF GAS TURBINE COMBUSTOR TURBULENCE

HOT COMBUSTOR TURBULENCE SPECTRA MEASUREMENTS OF MOSS AND OLDFIELD

LARGE SCALE ANNULAR COMBUSTOR MODEL OF AMES AND MOFFAT TURBULENCE IN THE HOT LINEAR CASCADE OF YORK, HYLTON AND MIHELC

LDA BASED TURBULENCE MEASUREMENT IN A MARQUARDT COMBUSTOR BY NIRMALAN AND HYLTON

TURBULENCE MEASUREMENTS IN A STRONGLY SWIRLING COMBUSTOR WITH NO DILUTION JETS, AHMED ET AL.

STUDIES RELATED TO THE EMULATION OF COMBUSTOR TURBULENCE USING PASSIVE AND ACTIVE GRIDS

PARALLEL HOLLOW BAR GRID WITH INJECTION

YOUNG AND HAN'S JET GRID FOR THE GENERATION OF HIGH TURBULENCE INTENSITIES

MEHENDALE, HAN AND OU'S JET GRID FOR HIGH TURBULENCE GENERATION

ACTIVE GRID USED BY GALASSI,KING AND ELROD
TURBULENCE PROMOTER USED BY KRISHNAMOORTHY AND SUKHATME
PASSIVE BIPLANE GRID USED IN DRING ET AL.'S TURBINE HEAT TRANSFER
EXPERIMENTS
PARALLEL BAR GRID OF MOSS AND OLDFIELD

TURBULENCE GENERATOR DESIGN (UNDER PROGRESS)

COMBUSTOR TURBULENCE ASSESSMENT TECHNIQUE (UNDER PROGRESS)

CURRENT TURBULENCE ASSESSMENT RESULTS (UNDER PROGRESS)

CONCLUDING REMARKS

REFERENCES

FIGURES

- APPENDIX A : Computer program calculating hot cascade total pressure for a prescribed cascade total temperature
- APPENDIX B : PROPGAS - A computer program for the generation of properties of natural gas/air combustion products
- APPENDIX C : A tabulation for the properties of natural gas/air combustion products from GORDON (1982)

ABSTRACT

The main goal of the present study is to present the principles used in the simulation of gas turbine flow and heat transfer fields in a hot cascade facility. The specific hot cascade facility is currently under operation at Solar Turbines Inc., San Diego. As far as the cascade total pressure and temperature is concerned the facility has the capability of running under full engine conditions. However, lower temperature operation is also possible by applying the rules of similarity. Mean flow and heat transfer similarity is achieved by replicating the Reynolds number, Mach number, and wall to free stream temperature ratio of the turbine. Local values at the inlet or exit of the vane/blade can be selected as simulation parameters. The annular cascade having four actual rotor blade passages is equipped with an actual combustor located upstream of the test section. Due to the existence of combustion products in the cascade, a very realistic simulation of the specific heat ratio and the molecular Prandtl number can be achieved. The paper presents the details of the procedure which is guaranteeing the mean flow/heat transfer similarity in the cascade. Coolant flow similarity is also discussed in detail.

Another goal of this document is to present the existing approaches for the generation and measurement of free stream turbulence in hot cascade research facilities. In the design of a hot cascade rig an important task is the simulation of the character of free stream turbulence existing in the actual engine combustor in addition to the conventional mean flow/heat transfer simulation parameters. Several previous studies dealing with the investigation of combustor turbulence are reviewed. Studies related to the generation of combustor turbulence using passive and active grids are also discussed.

NOMENCLATURE

SYMBOLS

A	area
c	chord length
D	diameter
Ec	Eckert number
g	gravitational constant
G	Grashof number
k	thermal conductivity
Ma	Mach number
m	mass flow rate
Nu	Nusselt number
P	pressure
Pr	molecular Prandtl number
Re	Reynolds number
S	a characteristic distance
T	temperature
U	absolute velocity
W	relative velocity at the turbine rotor exit

SUBSCRIPTS

w	wall
o	total,stagnation condition
∞	free stream condition
c	coolant condition
p	thermodynamic process at constant pressure
v	thermodynamic process at constant volume
tur	turbine condition
hc	hot cascade condition
hd	hydraulic diameter
inlet	inlet condition
slot	about the coolant slot
blade	about the blade

INTRODUCTION

The present study deals with the simulation of gas turbine flow and heat transfer fields in a hot cascade facility. The similarity ideas leading to the documentation of the simulation parameters are discussed in detail. A schematic of the hot cascade facility of Solar Turbines Inc. is shown in Figure 1. The facility operates from a large reservoir. A continuous operation under steady state conditions is possible. The combustor operating conditions can be adjusted in such a way that a wide operating temperature range from ambient conditions to full scale engine conditions is possible. Upstream and downstream pressure controller valves are capable of adjusting the cascade local flow conditions. The current test section in the hot cascade is from an existing engine (Mars). Five geometrically equivalent blades form a partial annular cascade with four blade passages. Figure 2 shows the current cascade arrangement. The blade located in the middle of the cascade is heavily instrumented for heat transfer research purposes. Preliminary results from total pressure and temperature measurements using 6 element rakes in the hot cascade are given in Figure 3 and 4. Figure 3 presents the hot cascade runs at low pressure (2.5 - 5.0 psig) with a wide total temperature range (400 - 800 F). Tests performed at a fixed combustor exit temperature (800 F) but in a wide total pressure range (2 - 33 psig) as shown in Figure 4 indicated that heightwise total pressure traverses taken using a dummy test section have a very uniform distribution. Corresponding Mach numbers at the inlet of the dummy test section were estimated to be between 0.12 and 0.32.

Recent research performed in the last few decades shows that convection heat transfer processes in a gas turbine engine are strongly altered/modified by free stream turbulence. The free stream turbulence experienced by the first set of nozzle guide vanes is originated in the combustor section. The rotors and stators located further downstream of the nozzle guide vanes experience a modified form of this combustor generated turbulence. Airfoil and endwall boundary layers of the nozzle guide vanes, the secondary flows in the nozzle passage, the corner vortices and the horseshoe vortex originating at the endwall/leading edge junction areas are important flow structures contributing to the generation/transport and dissipation of turbulent energy. Tip clearance flow and cooling jets discharging into the mainstream flow are additional factors

complicating the turbine passage flow. It should also be noted that the favorable pressure gradients existing on the curved surfaces of highly converging nozzle passages have a strong contribution on the structure of flow field discharging into the first stage rotor. The relative flow in the rotor also experiences the unsteady passage of wakes generated at the trailing edges of the nozzle guide vanes.

A very distinct response of laminar and transitional boundary layers to variations in free stream turbulence is a widely observed feature. In internal blade cooling arrangements, the amount of mixing in internal passages controls the heat transfer performance. Film cooling applied on the gas side of turbine airfoils is essentially a mixing process of cold and dense cooling jets and the hot free stream gases. This interaction may take place both in the hot gases of wall boundary layers or outside the boundary layer region if the momentum flux of the coolant jet is set to an extremely high level. High blowing rates cause the penetration of high density coolant jets into the free stream fluid. It is known that there is substantial augmentation of turbulent shear stresses at near downstream locations of film cooling row of holes.

Combustion of fuel and air mixture in a can type or annular combustor is controlled by atomization, evaporation and chemical reaction in a high pressure environment. Very pronounced turbulent mixing is a natural result of the flow/chemical reaction processes in a gas turbine combustor. Turbulent mixing in a combustor is also modified by the cooling/dilution jets originated at the walls of the flame tube. The secondary air jets ejecting into the combustor are necessary to keep the temperature distribution of the flame tube at a desired level. The mixing of the secondary jets within the hot combustor gases produces a significant portion of the free stream turbulence experienced in the nozzle guide vanes or in the passages located further downstream. Existence of swirl in modern combustors further complicates the structure of turbulence. The strong acceleration occurring near the exit section of the combustor also plays an important role in modifying the turbulence structure.

PRINCIPLES OF MEAN FLOW SIMILARITY IN THE HOT CASCADE RIG

An experimental investigation of forced convection heat transfer with and without film cooling across the boundary layers of a gas turbine blade should be carried out under well simulated conditions of the actual phenomenon. Schmidt (1963), Schlichting (1979) and Eckert and Drake (1972) evaluate the Navier-Stokes Equations and energy equation in a non-dimensionalized form, for a constant property compressible fluid. The solutions to these partial differential equations for laminar flow depend on a number of dimensionless groups. Non-dimensional form of the equations suggests that the similarity of fluid streamlines and the non-dimensional isothermal lines in the forced convection heat transfer field can be enforced by using the same magnitudes for these non-dimensional groups evaluated for both the actual phenomenon and the simulation experiment. When the steady forms of the momentum and energy equations are non-dimensionalized, the final solution fields strongly depend on the non-dimensional multipliers. Five major non-dimensional multipliers are given as follows.

$$\frac{\rho_{\infty} U_{\infty} S}{\mu}$$

$$\frac{g\beta (T_{\infty} - T_w) S}{U_{\infty}^2}$$

$$\frac{k}{\rho_{\infty} C_p U_{\infty} S}$$

$$\frac{U_{\infty}^2}{C_p (T_{\infty} - T_w)}$$

$$\frac{\mu U_{\infty}}{\rho_{\infty} C_p (T_{\infty} - T_w) S}$$

Since the fourth and fifth groups are dependent by factor of

$$\frac{\rho_{\infty} U_{\infty} S}{\mu}$$

only four non-dimensional quantities govern the similarity. The second group can be arranged as follows,

$$\frac{g\beta(T_{\infty} - T_w)S}{U_{\infty}^2} = \frac{g\beta S^3(T_{\infty} - T_w)}{v^2} \frac{v^2}{U_{\infty}^2 S^2} = \frac{G}{Re^2}$$

where G is the Grashof number.

$$G = \frac{g\beta S^3(T_{\infty} - T_w)}{v^2}$$

This non-dimensional group represents the ratio of inertia forces to buoyancy forces acting on an infinitesimally small fluid particle. For most of the forced convection problems such as heat transfer on a gas turbine blade buoyancy forces are considered negligible compared to inertia forces.

The third non-dimensional group can be rearranged as follows.

$$\frac{k}{\rho_{\infty} U_{\infty} C_p S} = \frac{k}{\mu C_p} \frac{\mu}{\rho_{\infty} U_{\infty} S} = \frac{1}{Pr} \frac{1}{Re}$$

The fourth non-dimensional group is known as the Eckert number.

$$Ec = \frac{U_{\infty}^2}{C_p(T_{\infty} - T_w)}$$

The Eckert number can be rearranged in terms of free stream Mach number, wall to free stream temperature ratio and specific heat ratio. The speed of sound propagation and equation of state can also be substituted into the equation defining the Eckert number.

$$a = (\gamma R T_{\infty})^{1/2}$$

$$a^2 = \gamma \frac{P_{\infty}}{\rho_{\infty}} = C_p (\gamma - 1) T_{\infty}$$

$$Ec = C_p (\gamma - 1) \frac{U_{\infty}^2}{a^2} \frac{T_{\infty}}{C_p (T_{\infty} - T_w)}$$

By non-dimensionalizing the temperature terms the Eckert number can be re-written.

$$Ec = (\gamma - 1) Ma^2 \frac{T_{\infty}/T_{\infty}}{1 - T_w/T_{\infty}}$$

The static to total temperature ratio can be replaced by using isentropic relations.

$$Ec = (\gamma - 1) Ma^2 \frac{\frac{1}{1 + \frac{(\gamma - 1)}{2} Ma^2}}{1 - \frac{T_w}{T_{\infty}}}$$

As a result of the rearrangements given up to this point, a forced convection heat transfer study dealing with the boundary layers developing on gas turbine blade surfaces requires the similarity of the following non-dimensional numbers.

Re	Pr	Ma	T _w /T _{infty}	C _p /C _v
----	----	----	------------------------------------	--------------------------------

The Nusselt number at the turbine exit location and at the hot cascade exit location will be similar if the similarity of the parameters given in the list is enforced. It should be noticed that this list results from the laminar/unsteady form of the momentum and energy equations. The same similarity argument could easily be implemented for the internal cooling passages of a typical gas turbine blade. Since the convective heat transfer process is from the wall to the coolant fluid, the temperature ratio (T_w/T_{∞}) should be replaced with a representative wall to coolant temperature (T_w/T_{oc}). All other parameters in the list should also be adjusted for the coolant flow conditions and coolant fluid properties.

The momentum and energy equations used in the current similarity argument were developed as laminar flow equations dealing with the mean flow structure. However, the character of free stream turbulence is also an additional heat transfer modifying factor. In order to complete the similarity argument, one should also simulate the free stream turbulence character of a gas turbine engine during heat transfer simulation experiments. Ideally, the intensity of free stream turbulence and a typical length scale of characteristic turbulent eddies should be provided in the simulation environment. It is a known phenomenon that turbulent flow imposes a slightly different momentum balance because of the existence of turbulent shear forces in addition to the shear forces of laminar flow due to molecular viscosity. An improved diffusion of mass and momentum in a fully turbulent near wall flow usually results in fuller boundary layer velocity profiles. Convective heat transfer to or from the wall is also enhanced due to additional fluid heat flux terms provided by the turbulent flow structure. A significant portion of the turbulent flow in the free stream of a gas turbine engine is generated in a combustor. The studies related to the character of combustor generated turbulence are reviewed in a different part of this paper.

When film cooling is applied, local heat transfer coefficients downstream of an injection hole are strongly affected by :

- coolant to free stream temperature ratio
- coolant to free stream mass flux rate ratio (blowing rate m)
- injection geometry

exit hole shape

- geometry of the hole cross section
- coolant trajectory in the hole
 - straight hole axis
 - curvilinear hole axis
- injection angle
 - slanted
 - compound angled
- cooling hole diameter to length ratio
 - hole spacing
 - row spacing
 - number of holes in one row
 - number of rows
 - row configuration
 - in-line rows
 - staggered rows
- pressure gradient along the injection site
- longitudinal curvature of the blade gas side surface
- surface roughness
- approaching gas side boundary layer character
- boundary layer displacement thickness to cooling hole diameter

SPECIFIC APPLICATION TO SOLAR HOT CASCADE FACILITY (GAS SIDE)

This section is about the implementation of the principles discussed in the previous section. The specific turbine configuration under simulation is a first stage rotor from one of the existing engines (MARS). The local Reynolds number at the exit of the rotor will be calculated and the exact same Reynolds number at the exit of the hot cascade will be imposed at the prescribed total temperature of the hot cascade. In summary, the user will be able to calculate the total pressure in the hot cascade at the prescribed hot cascade total temperature in such a way that the exit Reynolds number and Mach number in the turbine and hot cascade will be the same. The hot cascade test section under investigation is geometrically the same as the turbine rotor geometry. The known turbine conditions are :

- chord length
- relative velocity at the rotor exit
- static pressure and temperature at the turbine exit
- turbine total mass flow rate
- rotor throat area
- exit flow angle
- number of blades

Since the calculation of the local Mach number at the rotor exit requires the knowledge of fluid properties, a gas table for the natural gas/air combustion products will be used. Gas properties in U.S. customary units are given in Gordon (1982). A computer program which returns the properties at any prescribed temperature between 360 R and 5400 R has been developed under the name "PROPGAS". This program is listed in appendix B of this report. Appendix - C provides a tabulation of the gas table in detail. Reynolds number similarity between the turbine and the hot cascade requires the satisfaction of ,

$$\frac{\rho_{tur} W_{tur} c}{\mu_{tur}} = \frac{\rho_{hc} U_{hc} c}{\mu_{hc}}$$

where W_{tur} denotes the relative velocity at the turbine rotor exit and U_{hc} denotes the hot cascade absolute exit velocity. Relative Mach number at the exit of the turbine is defined as follows.

$$Ma = \frac{W_{tur}}{\sqrt{\gamma_{tur} R_{tur} T_{tur}}}$$

Density at the rotor exit can be obtained from the equation of state.

$$\rho_{tur} = \frac{P_{tur}}{R_{tur} T_{tur}}$$

Reynolds number at the turbine rotor exit can now be calculated.

$$Re_{tur} = \frac{W_{tur} \rho_{tur} c}{\mu_{tur}}$$

Total to static pressure ratio and temperature ratio at the exit of the turbine rotor can be calculated from isentropic relations.

$$\left(\frac{P_o}{P}\right)_{tur} = \left(1 + \frac{(\gamma_{tur}-1)}{2} Ma^2\right)^{\frac{\gamma_{tur}}{\gamma_{tur}-1}}$$

$$\left(\frac{T_o}{T}\right)_{tur} = \left(1 + \frac{(\gamma_{tur}-1)}{2} Ma^2\right)$$

Mass flux rate in the hot cascade exit station can be calculated from Reynolds number equation.

$$\rho_{hc} U_{hc} = \frac{\mu_{hc}}{\mu_{tur}} \rho_{tur} W_{tur}$$

Mass flux rate in the hot cascade exit station can also be evaluated starting from the equation of state and the definition of Mach number.

$$\rho_{hc} U_{hc} = \left(\frac{P_{hc}}{R_{hc} T_{hc}} \right) Ma \sqrt{\gamma_{hc} R_{hc} T_{hc}}$$

By equating the last two equations will provide an equation which enforces an exact Reynolds number similarity. Although the exit Mach number for the turbine shows up in the equation, the similarity of the Mach numbers at the turbine exit is not introduced into the analysis yet.

$$\frac{\mu_{hc}}{\mu_{tur}} \rho_{tur} W_{tur} = \left(\frac{P_{hc}}{R_{hc} T_{hc}} \right) Ma \sqrt{\gamma_{hc} R_{hc} T_{hc}}$$

At this stage we can easily replace the static temperature and the pressure in the cascade exit with the total pressure, total temperature and the imposed exit Mach number.

Static pressure in the hot cascade:

$$P_{hc} = \frac{P_{o,hc}}{\left(1 + \frac{(\gamma_{hc}-1)}{2} Ma^2 \right)^{\frac{\gamma_{hc}}{(\gamma_{hc}-1)}}}$$

Static temperature in the hot cascade:

$$T_{hc} = \frac{T_{o_{hc}}}{1 + \frac{(\gamma_{hc}-1)}{2} Ma^2}$$

One should notice that Ma is the same for both the turbine exit and the cascade exit. After substituting for the static temperature and pressure in the equation for the Reynolds number similarity, we can write the total pressure in the hot cascade facility in function of the total temperature in the hot cascade.

$$P_{o_{hc}} = \frac{\mu_{hc}}{\mu_{tur}} \frac{\rho_{tur} W_{tur}}{Ma \sqrt{\frac{\gamma_{hc}}{R_{hc}}}} \left(1 + \frac{(\gamma_{hc}-1)}{2} Ma^2\right)^{\frac{\gamma_{hc}}{\gamma_{hc}-1}} \sqrt{\frac{\frac{T_{o_{hc}}}{1 + \frac{(\gamma_{hc}-1)}{2} Ma^2}}{}}$$

The total pressure in the cascade can be calculated if the total temperature in the cascade is imposed. At this stage turbine conditions including the local Mach number and Reynolds number is known. Total temperature can easily be controlled by changing the combustor operating conditions. Calculation of the cascade total pressure requires a straight forward iteration procedure because the specific heat ratio and the gas constant in the hot cascade are not known

at the first step. Although the static temperature in the cascade is not known at this stage, total temperature is known. It is known that the gas constant does not show strong temperature dependency. However, the specific heat ratio has some non-negligible static temperature dependency. Since the hot cascade static temperature is not known initially, the fluid properties can be approximately evaluated at the turbine static temperature (rotor exit). This approach allows us to make our first approximate calculation of total pressure, static temperature and static pressure. At this stage there is some error in the three quantities calculated initially because of our first approximation made on the specific heat ratio and gas constant. The new static temperature T_{hc} is now much more accurate than our first approximation which is $T_{hc}=T_{tur}$. If one obtains the necessary properties with the new static temperature and recalculates the total pressure, static temperature and static pressure in the cascade, the new result will be much more accurate than the results obtained at the previous steps. If this process is repeated a few times until the properties converge into a stable value, an exact solution to the hot cascade total pressure can be obtained. The current calculations indicated that three iterations is more than enough for a completely converged solution.

The unknown quantities were also calculated without corrections on fluid properties. This numerically approximate procedure always resulted hot cascade Reynolds numbers which is 4-6 % less than the turbine rotor exit Reynolds number.

A computer program going through the calculations described in this section is given in appendix A of this report. The current version of this program follows the most accurate calculation of the total pressure using the described iteration procedure.

Density in the hot cascade can now be calculated from the equation of state.

$$\rho_{hc} = \frac{P_{hc}}{R_{hc} T_{hc}} = \frac{P_{o_{hc}}}{\left(1 + \frac{(\gamma_{hc}-1)}{2} Ma^2\right)^{\frac{\gamma_{hc}}{\gamma_{hc}-1}}} \frac{1}{R_{hc} T_{hc}}$$

Knowing Mach number and the static temperature allows us to calculate the local velocity at the exit of the cascade.

$$U_{hc} = Ma \sqrt{\gamma_{hc} R_{hc} T_{hc}}$$

Calculating the Reynolds number from final hot cascade values and showing that it matches the turbine Reynolds number is a numerical check on the similarity calculations. The hot cascade Reynolds number.

$$Re_{hc} = \frac{\rho_{hc} U_{hc} c}{\mu_{hc}}$$

Mass flow rate in the cascade can now be calculated in the hot cascade test section. It should be

$$m_{hc} = \rho_{hc} U_{hc} (AREA x \cos \beta) \left(\frac{4}{88} \right)$$

noted that the hot cascade has four blade to blade passages when compared to 88 passages (also blades) in the actual turbine configuration. It is also useful to note that the term "AREA" is not the throat area at the rotor exit. [Area x cos(beta)] is the actual throat area subject to mass flow rate calculations at the exit of the cascade section where beta is the exit flow angle. The final results from this discussion are presented in Figure 5. The imposed cascade temperature was varied in a range from 100 F to 2000 F. A hot cascade total pressure was calculated by using the

analysis described above. Figure 5 shows the variation of the cascade total pressure with respect to the cascade (imposed) total temperature for the specific simulation task (first stage rotor - Mars). Although the turbine rotor exit Reynolds number and the Mach number is fully simulated, at low temperature operation relatively lower cascade total pressures are required when compared to the turbine total pressure. When the cascade is operated at drastically low temperatures, although the Reynolds number and the Mach number is matched fully, the simulation of the specific heat ratio becomes more and more difficult, even with the actual combustion gases in the cascade test section. A perfect mean flow similarity satisfying Re_c , Pr_c , Ma_c , T_w/T_{∞} and C_p/C_v can only be obtained when the cascade total temperature is set to the actual relative total temperature of the rotor. When temperatures relatively lower than the turbine relative total temperature is used, the simulation of the specific heat ratio will become more and more difficult due to its temperature dependent nature. One should also notice that exit Mach numbers of the turbine and the cascade are only matched at one point. Local distributions of turbine rotor Mach number and the cascade Mach number should be closely investigated on the blade surfaces at least at the mid span.

SPECIFIC APPLICATION TO SOLAR HOT CASCADE FACILITY (COOLANT SIDE)

Similarity principles applied to the gas side of the hot cascade can also be implemented for the coolant side of the blade profile under investigation. It was mentioned that free stream to wall temperature ratio is the main non-dimensional parameter providing a simulation of the thermal energy exchange features in the turbine passage. In practice, usually one single average value for this ratio is used although the wall temperature or free stream gas temperature at the edge of the boundary layer may have spatial gradients. On the coolant side a quality thermal simulation will be driven by the coolant total temperature to wall temperature ratio. For simulation purposes one can provide the same ratio in the hot cascade as the ratio observed in the actual turbine. Again a typical ratio is used although the local coolant to wall temperature ratios may vary in the internal coolant passages. A final list of non-dimensional numbers which should be simulated on the coolant side of the cascade airfoil is as follows.

$$\text{Re}_c \quad \text{Pr}_c \quad \text{Ma}_c \quad T_w/T_{oc} \quad C_p/C_v$$

According to similarity rules derived from the laminar/steady forms of the momentum and energy equations, the specific list given above guarantees the similarity of the Nusselt number defined between the coolant side of the turbine blade and the coolant side of the hot cascade blade. A full similarity at only one point is enforced, (exit station). Mach number is kept in the list in case there are non-negligible compressibility effects in the coolant passage. However, if the specific design guarantees that the local Mach numbers in the coolant passages are less than 0.3 , this term may easily be dropped. Satisfaction of the coolant specific heat ratio and coolant Prandtl number is also required. It should be noted that these parameters are slightly temperature dependent. If the cascade tests are performed at very low temperatures compared to the turbine total temperature level some deviation from the actual flow similarity may be experienced. In general these errors will be minimized with increasing hot cascade or coolant temperatures. Of

course a full simulation of the turbine total temperature (relative stagnation temperature at the passage exit) will guarantee a perfect similarity in terms of the Prandtl number and the specific heat ratio.

All of the coolant side similarity considerations discussed here are implemented in a computer program which is listed in appendix A. In this approach similarity is enforced at a single point on the coolant side of the cascade vane. Engine coolant conditions are well documented in terms of the inlet total coolant to free stream temperature ratio at the vane root where the coolant fluid enters into the passage. In addition to knowing the coolant temperature at the root, the temperature rise in the coolant passage is well documented between the root and the exit slots located at the trailing edge. The temperature rise in the engine coolant passage is expressed as the ratio of the temperature rise normalized by the temperature difference between the engine relative total temperature and the coolant temperature at the root.

$$\epsilon = \frac{\Delta T_{oc_{tur}}}{(T_{o_{rel,\infty}} - T_{oc_{inlet}})_{tur}}$$

We will assume that the cascade coolant passage will experience a similar non-dimensional temperature rise. For the current blade cooling arrangement, coolant side Reynolds number is defined at the exit of the coolant passage. The coolant discharge is accomplished on the pressure side part of the trailing edge through 17 non-circular cross section coolant slots. Temperature rise in the cascade vane coolant channel is absolutely required in order to define the coolant Reynolds number at the exit of the coolant passage. The non-dimensional temperature rise in the cascade which is numerically the same as the turbine value is defined as follows.

$$\epsilon = \frac{\Delta T_{oc_{hc}}}{(T_{o\infty} - T_{oc_{inlet}})_{hc}}$$

Engine coolant mass flow rate is usually expressed as a fraction of the free stream mass flow rate. If we denote number of slots in one blade by N_{slot} and the exit area of one slot by A_{slot} , the coolant mass flux rate per blade in the engine with N blades can be expressed as follows.

$$(\rho_c U_c)_{tur} = \frac{\dot{m}_{c_{tur}}}{N_{slot} A_{slot} N_{blade}}$$

Local Reynolds number at the exit of the coolant passage in the turbine is defined as follows.

$$Re_{c_{tur}} = \frac{(\rho_c U_c)_{tur} D_{hd}}{\mu_{c_{tur}}}$$

where D_{hd} is the hydraulic diameter of one of the coolant slots located at the exit of the coolant passage. N_{slot} is 17 for the current blade under consideration. Since we are matching the Reynolds number and the coolant to free stream total (relative) temperature ratio of the engine in the hot cascade rig, we are required to calculate the coolant mass flux rate in the cascade to match the coolant Reynolds number of the engine under imposed cascade total temperature conditions.

$$(\rho_c U_c)_{hc} = (\rho_c U_c)_{tur} \frac{\mu_{c_{hc}}}{\mu_{c_{tur}}}$$

The difference in coolant mass flux rates between the cascade and the turbine is due to viscosity. Different total temperature conditions existing (imposed for the case of cascade) in the cascade and turbine result in significantly different absolute viscosities in the two configurations. The calculations show that the coolant viscosity difference is not negligible. Cascade coolant mass flow rate per blade can now be obtained from the mass flux rate.

$$(\dot{m}_c)_{hc} = (\rho_c U_c)_{hc} A_{slot} N_{slot}$$

Final results from the analysis providing the coolant flow similarity in the hot cascade facility is given in Figures 5 and 6. Again, the starting engine condition is the coolant side of the specific engine (Mars), first stage rotor. Required coolant temperature at the cascade vane root for similarity is plotted with respect to cascade total temperature in Figure 5. The required coolant mass flow rate for one blade in the cascade is also provided in Figure 6.

PAST WORK ON THE CHARACTERIZATION OF GAS TURBINE COMBUSTOR TURBULENCE

HOT COMBUSTOR TURBULENCE SPECTRA MEASUREMENTS OF MOSS&OLDFIELD:

Hot combustor turbulence measurements using a novel technique using dynamic pressure transducers were presented by Moss and Oldfield (1991). The measurements of turbulence spectra at the exit plane of three different aircraft combustors of the same family running at atmospheric exit pressure were discussed. They obtained turbulence wave number spectra for both hot and cold combustor flows. An uncooled dynamic pressure transducer mounted in a pitot probe configuration was injected into a hot combustor flow, Figure 7. The residence time of the probe in hot combustion gases was less than 100 milliseconds in a transient injection process of about two seconds. Temperature rise measurements of the diaphragm showed that most of the rise occurred after the probe has left the combustor. The probe temperature rise did not exceed 90 degrees C during the flight time inside the combustor. It was shown that the temperature rise of the dynamic pressure transducer during the transient injection experiment did not significantly influence the measured turbulence intensity. Tip of the turbulence measurement device showing the mounting of the dynamic pressure transducer is shown in Figure 8. The authors used a model based on the unsteady form of the Bernoulli's equation developed by Bradshaw (1971). The model uses a relationship based on the proportionality of the static pressure fluctuations and the dynamic head based on the fluctuating velocity as described by Hinze (1975). They also assumed that the density fluctuations due to compressibility at $Ma=0.25$ were negligible as opposed to temperature fluctuations. A final expression for turbulence intensity was simply expressed by scaling the dynamic stagnation pressure data. No significant differences between the cold and hot turbulence wave number spectra were observed, Figure 9. The experiments run in one combustor with four different fuel-air ratios with one fuel type produced very similar turbulence spectra. The spectral distributions obtained with different fuels (diesel and paraffin) at the same fuel air ratio were very close to each other as shown in Figure 10. Three different combustors with the same fuel at the same fuel air ratio were investigated. The spectras were so similar that the authors

concluded either that turbulence produced by the combustor head and the burner configuration was swamped by the turbulence generated far downstream by mixing of the dilution jets or that all three combustor flows produced very similar spectra, Figure 11. Moss and Oldfield (1991) concluded that the latter were less likely. It was claimed by the authors that these unexpected results may apply only to the particular combustor family exhausting to atmosphere. The spectras based on radial and axial components of the velocity fluctuations from cold tests were compared as shown in Figure 12. They found that at low wave numbers the radial fluctuating velocity component is smaller than the axial component. They interpreted this influence with the geometry of the discharge nozzle. At low wave numbers the discharge nozzle would be too narrow for the vortices to pass through. This would attenuate radial component but not the axial one. The comparison of the two spectras based on the radial and axial velocity component is given in Figure 12.

LARGE SCALE ANNULAR COMBUSTOR MODEL OF AMES&MOFFAT: The main objective of this study was to investigate the effect of combustor-like turbulence on both turbulent boundary layer and cylindrical stagnation region heat transfer, Ames and Moffat (1990). From the perspective of the exiting turbulent flow, the authors listed the critical features as the large scale recirculation in the primary zone, the penetration and mixing of jets in the dilution zone, and the contraction of the flow in the transition section. Their description of combustion flow fundamentals for modern annular combustors in a generic combustor is shown in Figure 13. The large scale recirculation in the primary zone was produced by a combination of primary jets and wall jets. The cross section of the turbulence generator was square. A swirler in the combustor was avoided because of an unacceptable production of mean rotation for boundary layer studies. The dilution jet penetration and mixing were simulated with one row of dilution holes. Finally a two to one area ratio nozzle contracted the flow. A schematic of the turbulence generator they built is shown in Figure 14. Five different versions of the turbulence generator were constructed with free stream velocity values varying from 6 m/s to 23 m/s. Typical turbulence intensities (based on the axial component) achieved with this arrangement varied between 8 % and 20 %. Figure 15 presents their streamwise turbulence intensity data for a combustor exit velocity of 6 m/s.

TURBULENCE IN THE HOT LINEAR CASCADE OF

YORK, HYLTON AND MIHELC: In a turbine end-wall heat transfer investigation, a combustor driven linear cascade facility was used by York et al. (1984). A gas fired Marquardt combustor provided a realistic simulation of the Mach number, Reynolds number, inlet boundary layer thickness, gas to wall temperature ratio, inlet pressure and temperature gradient. Test section temperatures of 800 ° C was possible. Typical combustor generated turbulence intensities in a range from 7.9 % to 9.35 % were generated. The specific combustor shown in Figure 16 did not have dilution/film cooling jets on the flame tube. The investigators could vary the free stream turbulent intensity by changing the burner operating point.

LDA BASED TURBULENCE MEASUREMENT IN A

MARQUARDT COMBUSTOR BY NIRMALAN AND HYLTON : A heat transfer study of film cooling on a turbine vane cascade was performed in the same combustor driven hot cascade facility used by York et al. A cascade exit Mach number range from 0.9 to 1.05 was generated at a free stream total temperature level of 700 K (802 F). A typical turbulence level measurement at the exit of the Marquardt combustor was reported as 6.5 % based on laser Doppler anemometer measurements, Nirmalan and Hylton (1990).

TURBULENCE MEASUREMENTS IN A STRONGLY SWIRLING COMBUSTOR WITH NO

DILUTION JETS, AHMED ET AL. (1992): Two component laser Doppler measurements at the exit section of a strongly swirling combustor having a diameter of 152 mm and a length of 1850 mm. was obtained. The combustor was directly discharging into a larger diameter pipe as shown in Figure 17. Typical combustor velocity was about 30 m/s at a Reynolds number level of 200,000 based on swirler outer diameter. They obtained turbulent intensities in all three directions at three different measurement stations. Measurements at the near field, mid field and far field were performed at ($x/D = 0.063 \dots 0.50$), ($x/D = 0.58 \dots 1.33$) and ($x/D = 1.66 \dots 4.00$), respectively. High values of turbulence intensities about 25% in the near field region were observed. In the mid field the turbulence intensities decayed into a range between 20-25 %. Finally, in the far field region typical levels between 5 - 10 % were observed. Their combustor had a 40 % contraction at the exit section without any dilution jets on the flame tube.

STUDIES RELATED TO THE EMULATION OF COMBUSTOR TURBULENCE USING PASSIVE AND ACTIVE GRIDS

PARALLEL HOLLOW BAR GRID WITH INJECTION: O'Brien and Vanfossen (1985) used an active grid with the compressed air flowing inside the hollowed parallel bars to generate high turbulence. The unidirectional parallel bars with injection jets flowing in the counter-flow (upstream) and co-flow (downstream) direction generated turbulence intensities as high as 15%. The turbulence intensity at 16 grid diameters downstream from the jet grid was 12% for co-flow injection with the injection ratio adjusted to an optimal value for flow uniformity.

YOUNG AND HAN'S JET GRID FOR THE GENERATION OF HIGH TURBULENCE INTENSITIES: The active grid used was a biplanar, square mesh, with 13 by 7 oriented aluminum tubes as described by Young and Han (1988). A solidity of 44% with a tube diameter of 0.635 cm was used.

The tube centerline spacing was 2.54 cm as shown in Figure 18. Each tube had 55 uniformly distributed injection holes with a hole diameter of 0.132 cm. The injection hole spacing was 2.54 cm in the counter-flow (upstream) direction. The same jet grid system was used for the downstream (co-flow) injection by rotating the grid 180 degrees. Four individually metered steel chambers were connected to the active grid. Streamwise turbulence intensities ranging from 3% to 20% were generated by using both counter-flow injection and co-flow injection through the grid system. They also documented the decay of streamwise turbulence for the case of no injection that was well documented from previous studies. The observed decay function agreed well with the data published by Blair et al. (1981), Figure 19. In the nearly isotropic region that was after the first 20 grid tube diameter distance, a turbulence intensity of 12% to 15% could be produced. The corresponding turbulence intensity with zero injection was 7 to 8%.

MEHENDALE, HAN and OU'S JET GRID FOR HIGH TURBULENCE GENERATION:

Mehendale et al. (1990) designed three different plane turbulence grids as shown in Figure 20. The first was a relatively low turbulence grid made of stainless steel bars (0.5×0.5) cm² of square cross section and 1.9 cm apart. A second grid was a passive grid made of hollow brass tubes (1.3×1.3) cm² in cross section and 4.8 cm apart. This passive grid also served as the jet grid as it had 96 holes, each 0.5 mm in diameter. The injection holes facing downstream were located at the grid nodes in the vertical tubes. These vertical tubes were connected at the top and bottom to two injection plenums. The bar grid generated streamwise turbulence intensity varied between 3.3 and 5.1 %. However the passive grid and jet grid generated relatively higher turbulence levels, (7.6 . . . 9.7) % and (12.9 . . . 15.2) %, respectively. The streamwise decay of turbulence was fully documented in this study for all three turbulence grids. The most significant decay in all grids was observed in the first 20 grid widths measured from the grid location, Figure 21. A very interesting feature of this study was the consistency of the current heat transfer results obtained under elevated turbulence intensity conditions with that of the correlations given by Lowery and Vachon (1975) developed under low turbulence intensity conditions. The two classical correlations for both the stagnation point and the averaged leading edge Nusselt number were in excellent agreement with the new experiments of Mehendale et al. (1990). The two correlations are as follows,

$$\text{Nu}_D / (\text{Re}_D)^{1/2} = 1.010 + 2.624 [\text{Tu}(\text{Re}_D)^{1/2}/100] - 3.07[\text{Tu}(\text{Re}_D)^{1/2}/100]^2$$

(Stagnation Point)

$$\text{Nu}_D / (\text{Re}_D)^{1/2} = 0.902 + 2.140 [\text{Tu}(\text{Re}_D)^{1/2}/100] - 2.89[\text{Tu}(\text{Re}_D)^{1/2}/100]^2$$

(Overall leading edge)

Figure 23 shows the stagnation point correlation in function of the turbulence intensity and the Reynolds number based on the cylinder diameter. The circular symbols show a Nusselt number variation with a maximum located at $\text{TU}^* \text{Re}^{1/2} = 40$. The part of this second order curve with a positive slope is an excellent match to some heat transfer data taken at $\text{TU}^* \text{Re}^{1/2} < 40$. Most of the wind tunnel experiments with a turbulence intensity value up to 15 % fall into this

category which is marked as region A in Figure 23. However, typical actual combustion exit values for $TU^*RE^{1/2}$ is greater than 40 and possibly less than 100. Region B in Figure 23 shows this gas turbine related region. It is clear that using the part of the Nusselt number curve with negative slope will introduce non-negligible errors into the heat transfer prediction. It is suggested that, until some real observation is made in region B, an extrapolation of the existing data from region A is used for hot cascade heat transfer prediction purposes.

ACTIVE GRID USED BY GALASSI, KING AND ELROD: In a study dealing with the effects of inlet turbulence scale on blade surface heat transfer in a linear cascade, Galassi et al. (1990) employed the active grid designed by Young and Han (1988). The turbulence integral scale and microscale lengths of the free stream flow were controlled by air injection from the jet grid. They used three sets of hollow tubes (0.635 cm) with different injection orifice diameters, (0.66 mm, 1.32 mm, 1.98 mm). Variation of turbulence was accomplished by adjusting the injection pressure, and the direction of injection. The three injection directions are the streamwise direction (co-flow), normal direction (cross-flow), opposite to the flow as shown in Figure 22. The investigators also placed the active grid at two different streamwise locations. The streamwise turbulence intensities were in a range between 6 % and 13 %. The cross stream turbulence intensity was varying between 4 % and 11 %.

TURBULENCE PROMOTER USED BY KRISHNAMOORTHY & SUKHATME :

Krishnamoorthy and Sukhatme (1980) established a new type of active turbulence promoter in a study to investigate the effect of free stream turbulence on gas turbine blade heat transfer. Their documentation on the high level of free stream turbulence in a gas turbine engine was based on the study published by Kurosh and Epik (1970). They constructed their promoter with a single hollow tube in which two rows of holes of 1 mm diameter and 2 mm pitch were drilled along the axial direction. However, the two injection rows were 180 degrees apart from each other. They located the turbulence generator hollow tube at a distance 625 mm upstream of the cascade inlet with its axis in the blade spanwise direction. The rotor blade chord length was given as 5.04 cm. The turbulence at the cascade inlet was varied by varying the injection pressure. They reported a measured integral length scale of 2.6 mm. The integral length scale did not change significantly with the free stream turbulence intensity level. The diameter of the single promoter pipe is not given. The authors claimed that the turbulence intensity was uniform along the height of the cascade. However no explanation was given for the uniformity of the streamwise turbulence intensity along the direction normal to the turbulence promoter and the inlet flow direction. A very wide range of turbulence intensities from 1.6 % up to 21.3 was reported.

PASSIVE BIPLANE GRID USED IN DRING ET AL.'S

TURBINE HEAT TRANSFER EXPERIMENTS: Dring et al. (1986) in this research effort first considered unidirectional bar arrays. They rejected this configuration because of the anisotropic character of turbulence downstream of the grid. They also rejected active grids with injection because of the uncertainty of the published data during their research period. Recently, a reliable group of published papers proved that active grids with jet injection were the most successful way of generating turbulence levels between 10 % and 20 %. Dring et al. also claimed that by using a perforated plate it was possible to achieve high levels of turbulence. However, due to the fast decaying character of streamwise turbulence, this configuration was not widely used. Finally a biplane passive grid was chosen as the turbulence promoter of the Large Scale Low Speed Turbine Research Facility at the United Technologies Research Center. Details of square array biplane lattice of square cross section bars are given in Comte-Bellot and Corrsin (1966), Hancock (1980,1983) and Blair et al. (1981). The grid was made of three uniformly spaced rings

of square cross section (1.27cmx1.27cm). 80 radial bars were also used to provide the biplane character of this turbulence generator. The distance between the ring centerlines was 5.33 cm. This arrangement provided a 5.33 cm spacing between the two subsequent radial bars at the mid span of the grid. They observed a short length of turbulence development region. The grid was placed in a way that the turbulence development region ended upstream of the test section. It was also made sure that the rate of decay of turbulence is not fast through the test section. The grid to test section distance was 38.1 cm corresponding to - 23 % chord distance upstream of the vane leading edge as shown in Figure 24. By using the correlation developed by Baines and Peterson (1951), they predicted that the streamwise turbulence intensity would decrease from 10 % to 5 percent between the first vane leading edge and the second vane trailing edge. Streamwise turbulence intensity at $x=-3.43$ cm (6.5 mesh width distance measured from the grid) is given in Figure 25 in function of spanwise distance. Their experimental results showed that the streamwise turbulence intensity decay function was as follows.

$$u'/U = 1.12(x/b)^{-5/7}$$

This correlation was in excellent agreement with the data provided by Baines and Peterson (1951), Figure 26.

PARALLEL BAR GRID OF MOSS AND OLDFIELD: Effects of free stream turbulence scale on heat transfer on a flat plate were studied by Moss and Oldfield (1992) in a streamwise turbulence intensity range greater than 7 %. They focussed on generating free stream turbulence levels greater than 10 % that is a typical value for an aircraft engine combustor exit. They also predicted that, in general, turbulence levels in HP turbines are less than 20 %. Their turbulence generator was made of circular cross section solid bars having 6, 60 and 15 mm diameter bars to generate different turbulence intensity levels. They also varied the grid model distance and the pitch of the bars in the grid. A set of streamwise turbulence intensity values and the corresponding integral length scales are given in table 1. They concluded that an accurate prediction of heat transfer enhancement due to free stream turbulence was not possible using the turbulence level alone. They provided a correlation to predict high pressure nozzle guide vane heat transfer enhancement from the local free stream turbulence intensity and length scale. The correlation is in good agreement with the data given by Hancock and Blair (1981).

CONCLUDING REMARKS

A detailed discussion of the similarity ideas applied on the gas side and coolant side of a typical gas turbine vane/blade is provided. A simple computer program to calculate the total pressure in the hot cascade for a prescribed total temperature is presented. The program with enough documentation lines is given in Appendix-A. The similarity approach used in this text makes use of accurate gas properties very frequently. In order to improve accuracy, a complete gas table in a static temperature range from 0 F to 5000 F is provided in Appendix-B in the form of a Fortran subroutine which may be used for other engine related flow/heat transfer problems.

The similarity of Reynolds number and Mach number at the exit section of the rotor passage is enforced. Leaving the total temperature in the cascade as a prescribed quantity is extremely helpful in matching a typical wall to gas total temperature of the turbine. Although the cascade can operate under full engine conditions, operation at reduced total pressure/temperature is possible. Cascade exit Reynolds number and Mach number can still be matched to that of the turbine. One minor problem with reduced total pressure operation is the difficulty of matching the specific heat ratio of the cascade and the turbine when the cascade is operating with the exact same combustion products of the turbine engine. For example when a specific heat ratio of 1.377 is typical at 100 F cascade operation, a specific heat ratio of 1.281 will be a corresponding full scale engine value for 1900 F.

Simulation of the coolant side heat transfer is also discussed in parallel gas side heat transfer similarity. The specific simulation point is chosen at the exit of the coolant slots. Coolant inlet temperature and the mass flow rate providing full mean flow/heat transfer similarity is presented for the prescribed cascade gas total temperature. A non-dimensional coolant temperature rise is used for the cascade coolant temperature rise between the root and the trailing edge slot exit location. The coolant side similarity ideas are also incorporated into the computer program given in Appendix-A. A summary of the main results for the specific turbine configuration (Mars) for the coolant simulation study is given in Figures 5 and 6.

Number of past studies related to the character of gas turbine engine turbulence generated in a combustor is limited. This study presents a recent literature review to form a current knowledge base in the area of combustor turbulence. Existing information from the recent studies and the present in-house measurements of free stream turbulence is expected to support the realistic simulation of engine flow conditions in the hot cascade facility of Solar Turbines Inc., San Diego.

Recent results obtained from three different aircraft engine combustors of the same family showed that slight variations in the geometrical definition of the combustor did not significantly alter the turbulence structure experienced by the nozzle guide vanes, Moss and Oldfield (1991). Two different fuels in the same combustor at the same fuel air ratio also generated similar turbulence spectras. A significant observation made by the same authors was the fact that the turbulence intensity contribution of the primary combustion zone is almost swamped by the strong hydrodynamic modifications of the dilution jets before the converging combustor exit

section. When the fuel air ratio was altered in the same combustor with the same fuel, similar turbulence spectra results were obtained. A cold test run also produced a turbulence spectra very similar to the first three experiments with combustion. The specific investigation is extremely valuable in documenting combustor turbulence. However, some caution should be exercised due to the fact that the specific combustors directly discharged into the atmosphere rather than discharging into a pressurized environment. Many assumptions made during the extraction of turbulence information from dynamic pressure data should also be questioned further for their validity in a wide range of operating conditions.

In a basic study, Ames and Moffat (1990) designed a large scale combustor cold flow model to generate realistic turbulence for nozzle guide vane heat transfer studies. They generated a wide turbulence intensity range from 8 to 20 percent by using the geometrical variations of the same combustor model. However, they neither had a swirling primary zone nor the actual combustion process. Their cold model had a square cross section in contrary to many round shaped can combustors or smoothly curved annular combustors existing in actual systems. The system certainly generated high turbulence intensities. However, matching the turbulence spectra of a real combustor was not investigated in this specific study.

Streamwise turbulence intensity levels from 6.5 % to 9.35 % were reported by York et al. (1984) from a Marquardt combustor driven hot cascade. The specific combustor operating under realistic engine temperature conditions did not have dilution jets. The turbulence intensity levels less than 10 % with full primary combustion could be attributed to the simplicity of the combustor without dilution jets as significant turbulence promoters. Another interesting feature of the combustor was the variation of turbulence intensity with changed fuel-air ratio. This observation is in contrast to the aircraft engine combustor results from Moss and Oldfield (1991). However, Moss and Oldfield's combustor is a full scale engine combustor with dilution jets that are dominating the turbulence field.

Finally, turbulence measurements from a strongly swirling combustor without dilution jets showed that near field ($x/D=0.063 - 0.50$), mid field ($x/D=0.58 - 1.33$) and far field ($x/D=1.66 - 4.00$) turbulence intensities were around 25 %, 20-25 % and 5-10 % respectively, Ahmed et al. (1992).

All of the combustors reviewed up to this point used an approximate 50 % contraction at the exit section. A common feature of most of the observations was the existence of a common turbulence intensity range of 10-15 % at approximately 2 combustor diameter downstream of the fuel injector location. Combustors without dilution jets produced relatively lower turbulence intensities (6-9 %) at the same location.

Five different active grids using jets in biplane or uni-plane mode and 2 passive grids were investigated in terms of their capabilities to generate combustor like turbulence. All seven grids could generate turbulence intensities between 6-20 %. Geometrical definitions and decay characteristics of these grids were documented for future turbulence generation efforts in the hot cascade facility.

It was a known fact that stagnation region heat transfer on a cylinder correlated with streamwise turbulence intensity at low and moderate turbulence intensity levels ($TU < 5\%$). One recent study showed that the same correlation could be used when turbulence intensities are above 5 % up to 13 %. The availability of a stagnation region heat transfer correlation for high turbulence intensities prompted the design of a turbulence measurement device using the cylinder in cross flow correlation. The current turbulence measurement device designed for use in the hostile environment of the hot cascade rig is based on stagnation heat flux measurements with reasonable accuracy.

REFERENCES

- Ahmed, S.A., Rose, A., Nejad, A.S., 1992, "Three Component LDV Measurements in a Can Type Research Combustor for CFD Validation, Part-1 Isothermal," ASME paper 92-GT-138, Presented at the International Gas Turbine Congress, Cologne, Germany.
- Ames, F.E. and, Moffat, R.J., 1990, "Heat Transfer with High Intensity, Large Scale Turbulence : The Flat Plate Turbulent Boundary Layer and the Cylindrical Stagnation Point," Report No. HMT-44, Thermosciences Division, Dept. of Mechanical Engineering, Stanford University.
- Baines, W.D. and Peterson, E.G., 1951,"An Investigation of Flow Through Screens," Trans. ASME, Vol.73, pp.467-480.
- Blair, M.F., Bailey, D.A. and Schlinker, R.H.,1981,"Development of a Large Scale Wind Tunnel for the Simulation of Turbomachinery Airfoil Boundary Layers," ASME Journal of Engineering for Power, Vol.103, pp.678-687.
- Comte-Bellot, G. and, Corrsin, S., 1966,"The Use of A Contraction to Improve Isotropy of Grid Generated Turbulence," Journal Of Fluid Mechanics, Vol.25, pp.657-682.
- Dring, R.P., Blair, M.F., Joslyn, H.D., Power, G.D., Verdon, J.M., 1986,"The Effects of Inlet Turbulence and Rotor/Stator Interactions on the Aerodynamics and Heat Transfer of a Large-Scale Rotating Turbine Model," NASA Contractor Report 4079, I-Final Report.
- Eckert, E.R.G. and Drake, R.M., 1972,"Analysis of Heat and Mass Transfer," McGraw Hill Book Company, pp. 389-397.
- Galassi, L., King, P.I. and Elrod, W.C., 1990,"Effects of Inlet Turbulence Scale on Blade Surface Heat Transfer in a Linear Cascade," AIAA paper 90-2264, presented at the 26 Th Joint Propulsion Conference, Orlando, FL.
- Gordon, S., 1982,"Thermodynamic and Transport Combustion Properties of Hydrocarbons With Air, III-Properties in U.S. Customary Units," NASA Technical Paper 1908.
- Hancock, P.E., 1980,"Effect of Free Stream Turbulence on Turbulent Boundary Layers," Ph.D. Thesis, Imperial College, University of London.
- Hancock, P.E. and, Bradshaw, P., 1983,"The Effect of Free Stream Turbulence on Turbulent Boundary Layers," ASME Journal of Fluids Engineering, Vol.105, pp.284-289.

Kurosh, V.D. and, Epik, E.Y., 1970,"The Effect of Turbulence on Heat Transfer in Turbomachinery Flow Passages," Heat Transfer-Soviet Research, Vol.2, No.1.

Lowery, G.W. and, Vachon, R.I., 1975,"The Effect of Turbulence on Heat Transfer from Heated Cylinders," International Journal of Heat and Mass Transfer, Vol.18, pp.1229-1242.

Mehendale, A.B., Han, J.C. and Ou, S., 1990,"Influence of High Mainstream Turbulence on Leading Edge Heat Transfer," Submitted to ASME Transactions, Journal of Heat Transfer. Also see Tech.Rep. RF-6475, Wright Patterson AFB.

Moss, R.W. and, Oldfield, L.G., 1992,"Measurements of Free-Stream Turbulence Length Scale on Heat Transfer," ASME paper 92-GT-244, Presented at the International Gas Turbine and Aeroengine Congress, Cologne, Germany.

Moss, R.W. and, Oldfield, L.G., 1991,"Measurements of Hot Combustor Turbulence Spectra," ASME paper 91-GT-351, Presented at the International Gas Turbine and Aeroengine Congress, Cologne, Germany.

Nirmalan, V. and, Hylton, L.D., 1990,"An Experimental Study of Turbine Vane Heat Transfer with Leading Edge and Downstream Film Cooling," ASME Transactions, Journal of Turbomachinery, Vol.112, pp:477-487.

O'Brien, J.E. and, VanFossen, G.J., 1985,"The Influence of Jet Grid Turbulence on Heat Transfer from the Stagnation Region of a Cylinder in Cross Flow," ASME paper 85-HT-58.

Schmidt, E., 1963,"Einfuhrung in die technische Thermodynamik und in die Grundlagen der Chemischen Thermodynamik," 10 th ed., Berlin,1963.

Schlichting, H., 1979,"Boundary Layer Theory," Seventh edition, McGraw Hill Co., pp 271-275.

York, R.E., Hylton, L.D., Mihelc, M.S., 1984,"An Experimental Investigation of Endwall Heat Transfer and Aerodynamics in a Linear Vane Cascade," Transactions of the ASME, Journal of Engineering for Gas Turbines and Power, Vol.106, pp:159-167.

Young, C.D. and, Han, J.C., 1988,"Effect of Jet Grid Turbulence on Turbulent Boundary Layer Heat Transfer," ASME bound volume HTD- Vol.103, Heat Transfer in Gas Turbine Engines and Three Dimensional Flows.

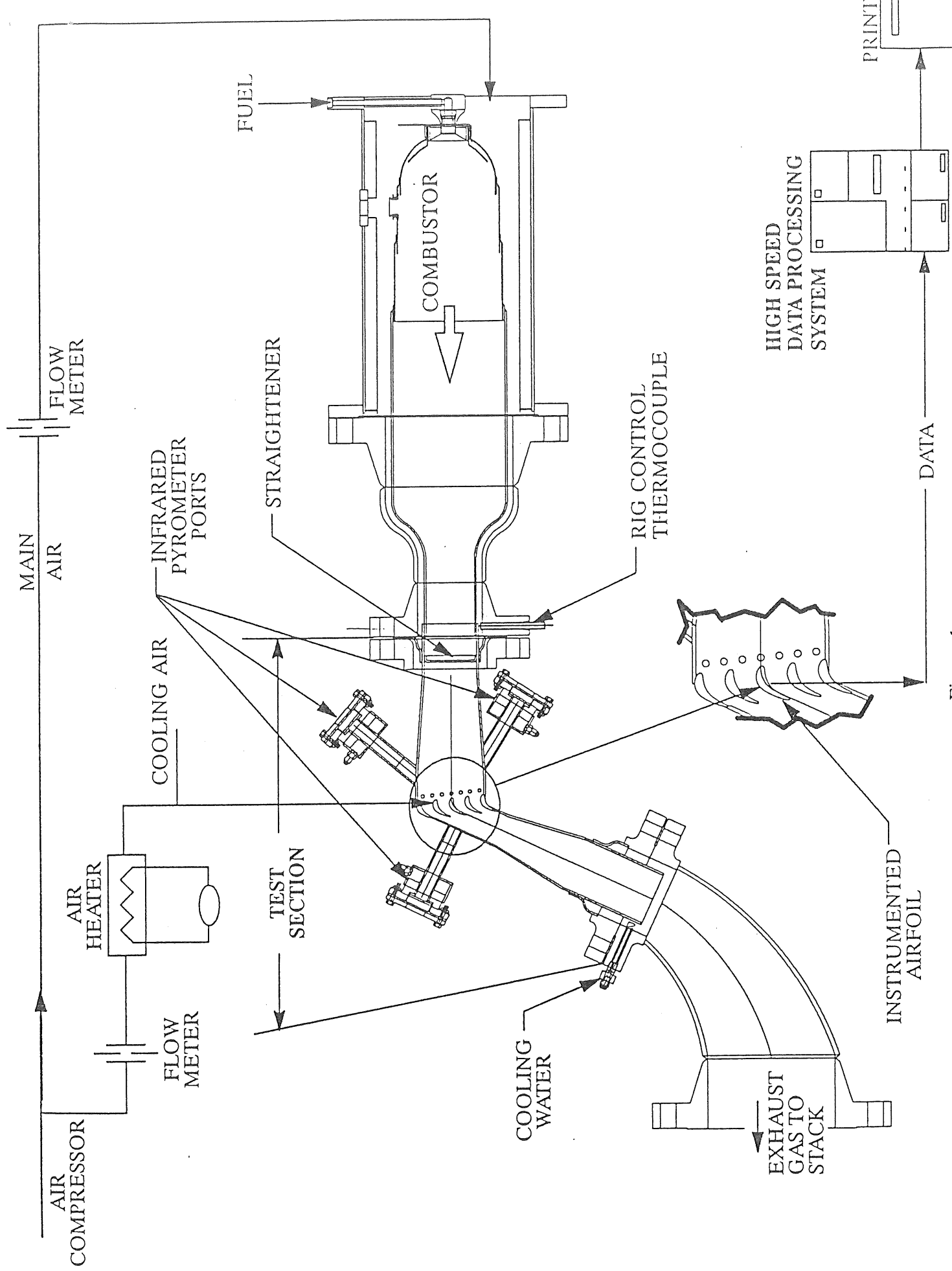


Figure 1

TURBINE AIRFOIL CASCADE TEST RIG

FIGURES

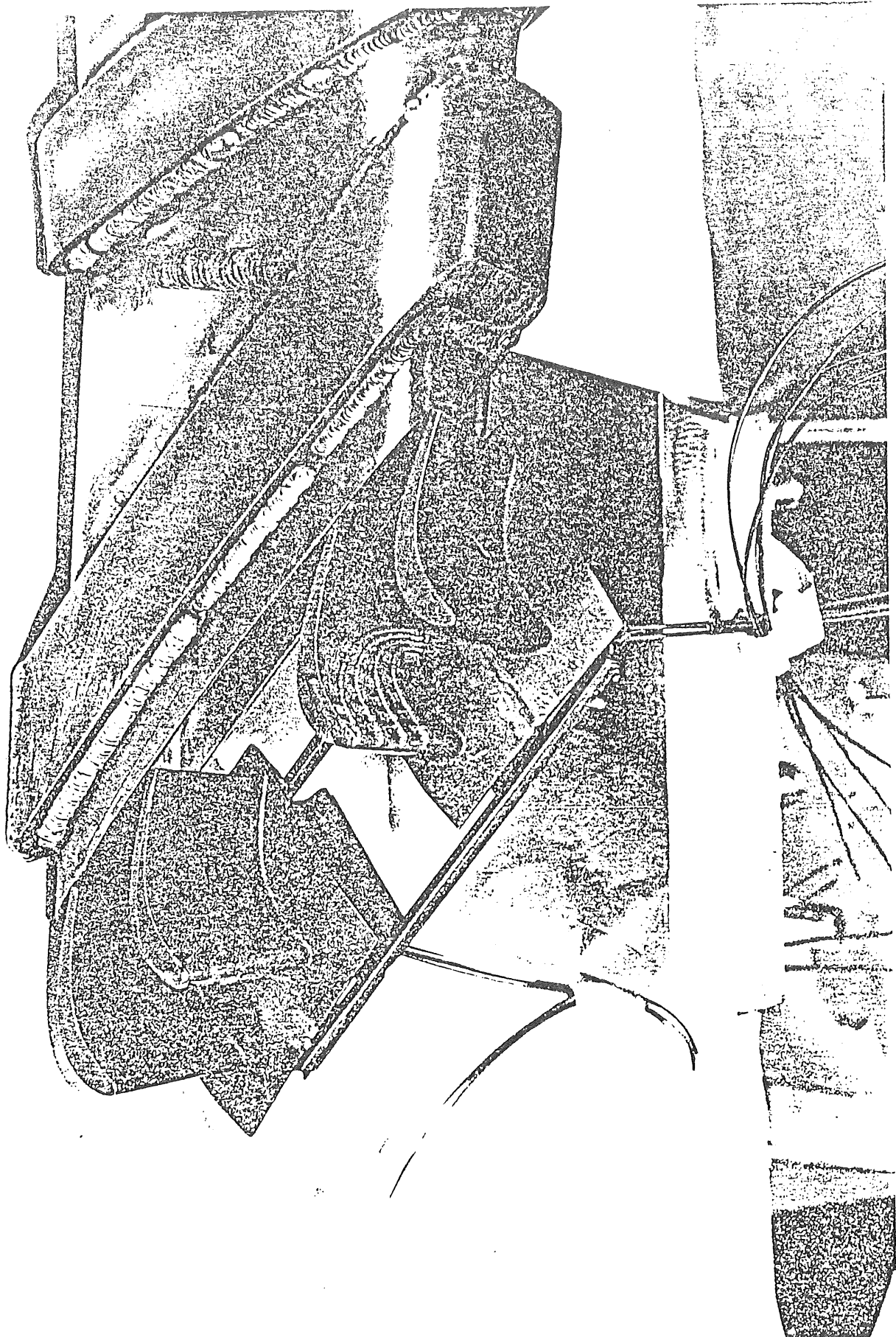
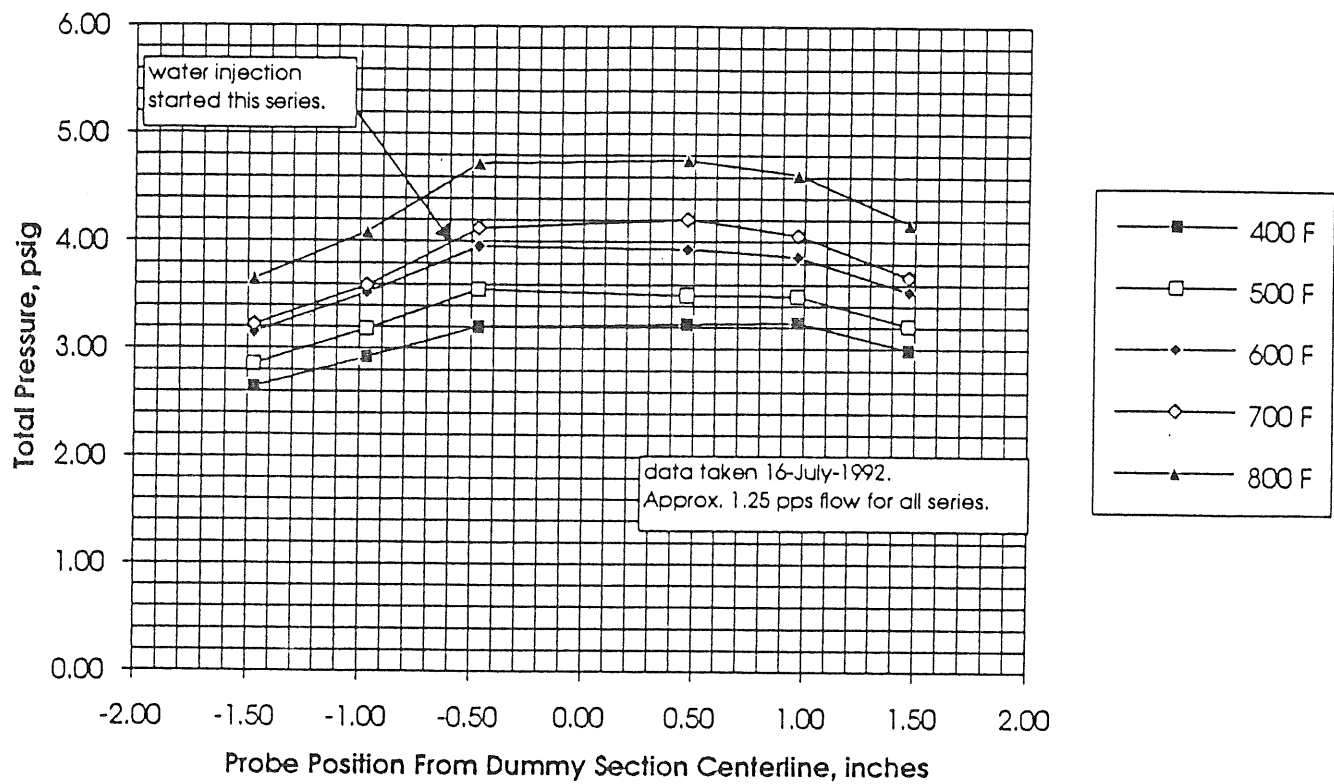


Figure 2

Hot cascade test section

Cascade Rig - Total Pressure Profile

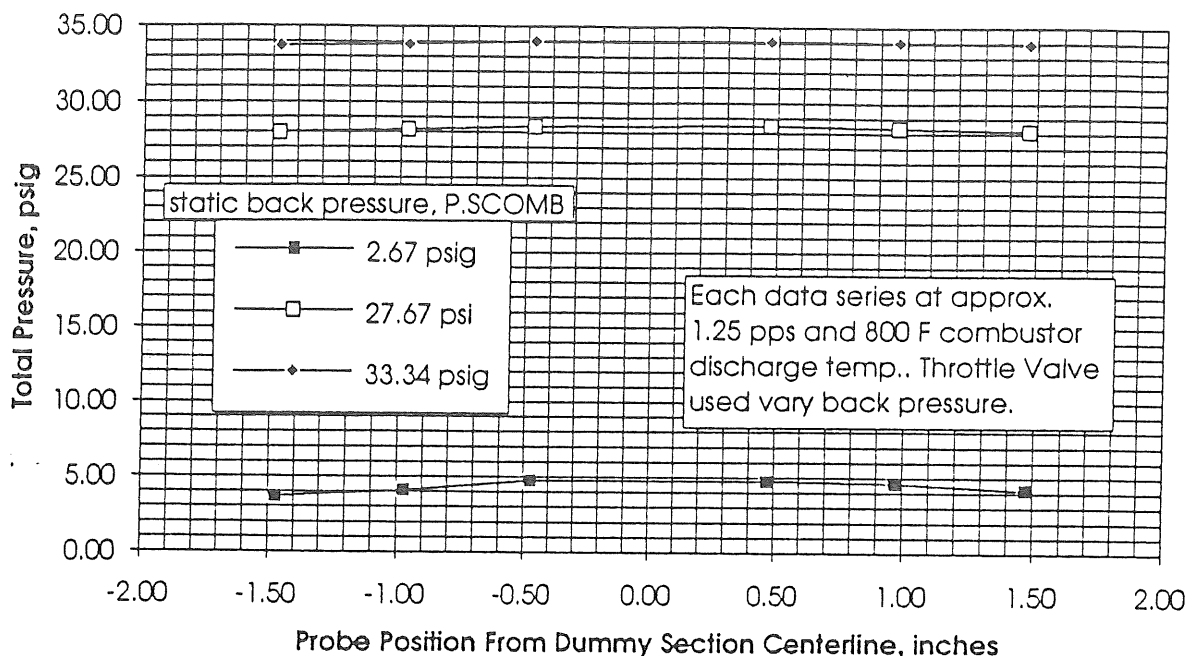


DATE	16-Jul-92	16-Jul-92	16-Jul-92	16-Jul-92	16-Jul-92			
TIME	14:37:54	14:42:07	14:45:29	14:55:00	14:59:11			
RUN.#	1	2	3	5	6			
Position								
P.RAKEB3	1.47	2.99	3.21	3.53	3.67	4.17		
P.RAKEB2	0.97	3.25	3.49	3.86	4.05	4.62		
P.RAKEB1	0.47	3.23	3.50	3.93	4.21	4.76		
P.RAKEA1	-0.47	3.20	3.55	3.95	4.12	4.73		
P.RAKEA2	-0.97	2.92	3.18	3.52	3.59	4.09		
P.RAKEA3	-1.47	2.65	2.85	3.15	3.22	3.65		
P.SCOMB		1.932	2.095	2.347	2.353	2.67		
PS.IN.AV		10.58	11.53	12.87	14.42	15.93		
T.COMB.2		403.6	503.8	611.8	703.3	807.9		
T.RAKE1		353.1	447.0	505.7	594.0	731.0		
T.RAKE2		363.6	463.8	526.2	614.0	749.7		
TVLV.AV		373.1	444.2	535.0	301.3	397.9		
W.COMB		1.253	1.241	1.239	1.251	1.256		
W.OVB		0.041	0.043	0.046	0.048	0.051		
Ma., approx.		0.27	0.28	0.30	0.31	0.32		

Figure 3

Hot cascade total pressure profile
low pressures, wide temperature range

Cascade Rig - Total Pressure Profile



DATE		16-Jul-92	16-Jul-92	16-Jul-92				
TIME		14:59:11	15:22:57	15:30:41				
RUN.#		6	7	8				
Position								
P.RAKEB3	1.47	4.17	28.16	33.92				
P.RAKEB2	0.97	4.62	28.34	34.03				
P.RAKEB1	0.47	4.76	28.45	34.09				
P.RAKEA1	-0.47	4.73	28.39	34.04				
P.RAKEA2	-0.97	4.09	28.17	33.81				
P.RAKEA3	-1.47	3.65	27.96	33.67				
P.SCOMB		2.67	27.621	33.341				
PS.IN.AV		15.933	31.521	36.872				
PS.VLV.1		2.72	27.652	33.363				
T.COMB.2		807.858	815.182	788.388				
T.RAKE1		731.032	689.848	738.674				
T.RAKE2		749.712	705.75	747.826				
TVLV.AV		397.889	503.043	517.279				
W.COMB		1.256	1.245	1.261				
W.OVB		0.051	0.075	0.083				
Ma., Approx		0.32	0.13	0.12				

Figure 4

Hot cascade total pressure profile
800 F, wide pressure range

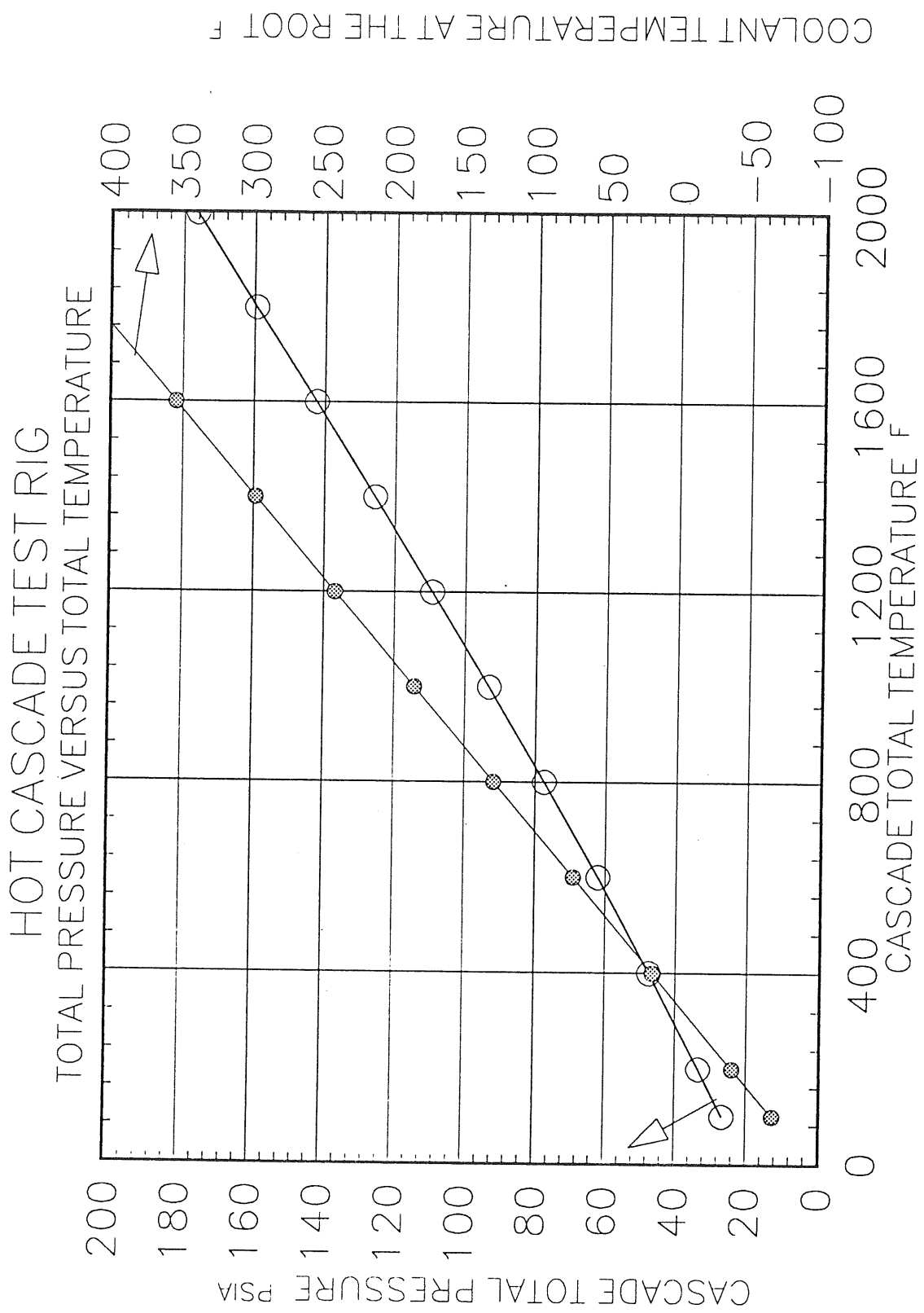


Figure 5

Variation of cascade total pressure
and coolant temperature at the root
with respect to cascade total temperature

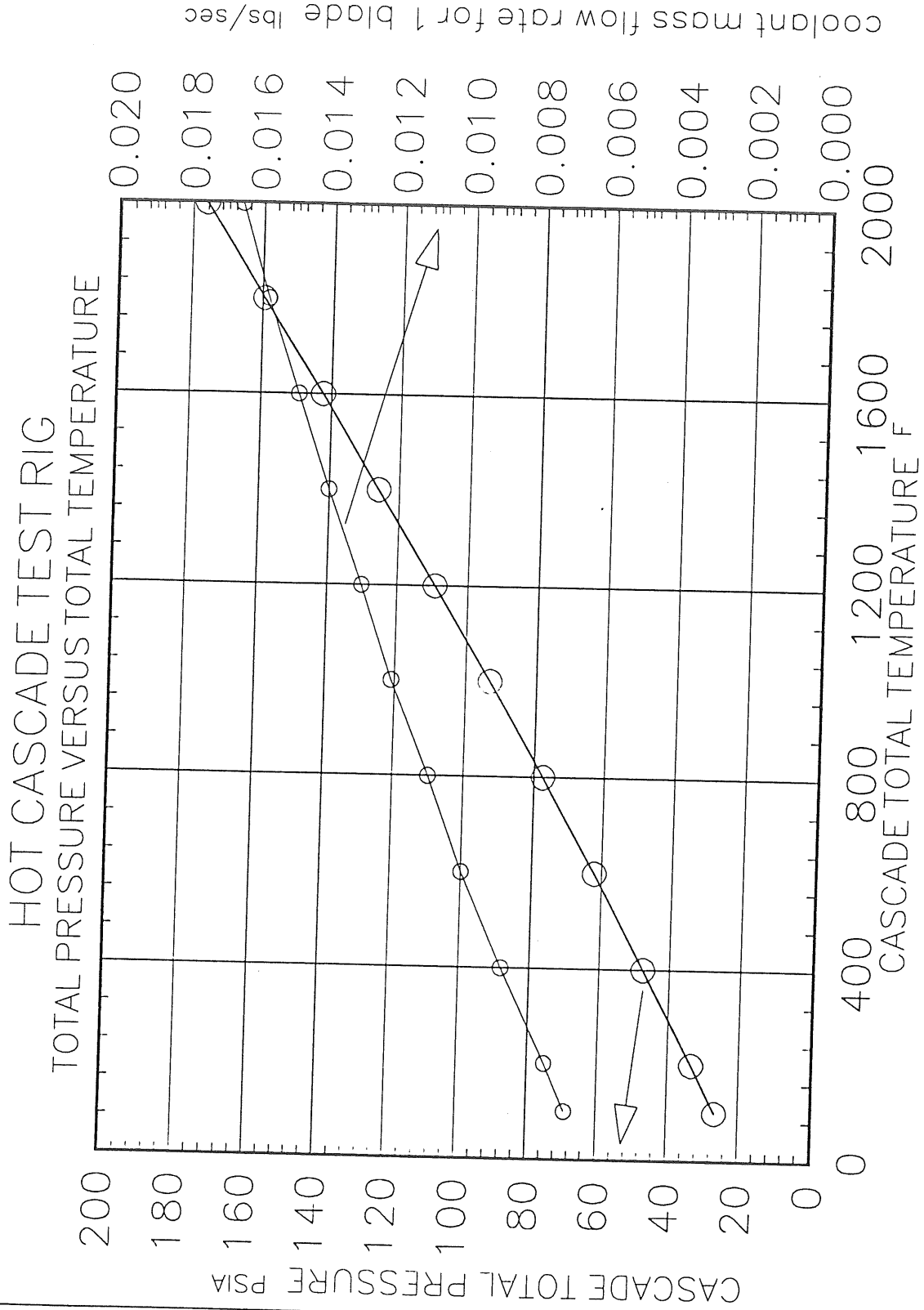


Figure 6

Variation of cascade total pressure
and coolant mass flow rate
with respect to cascade total temperature

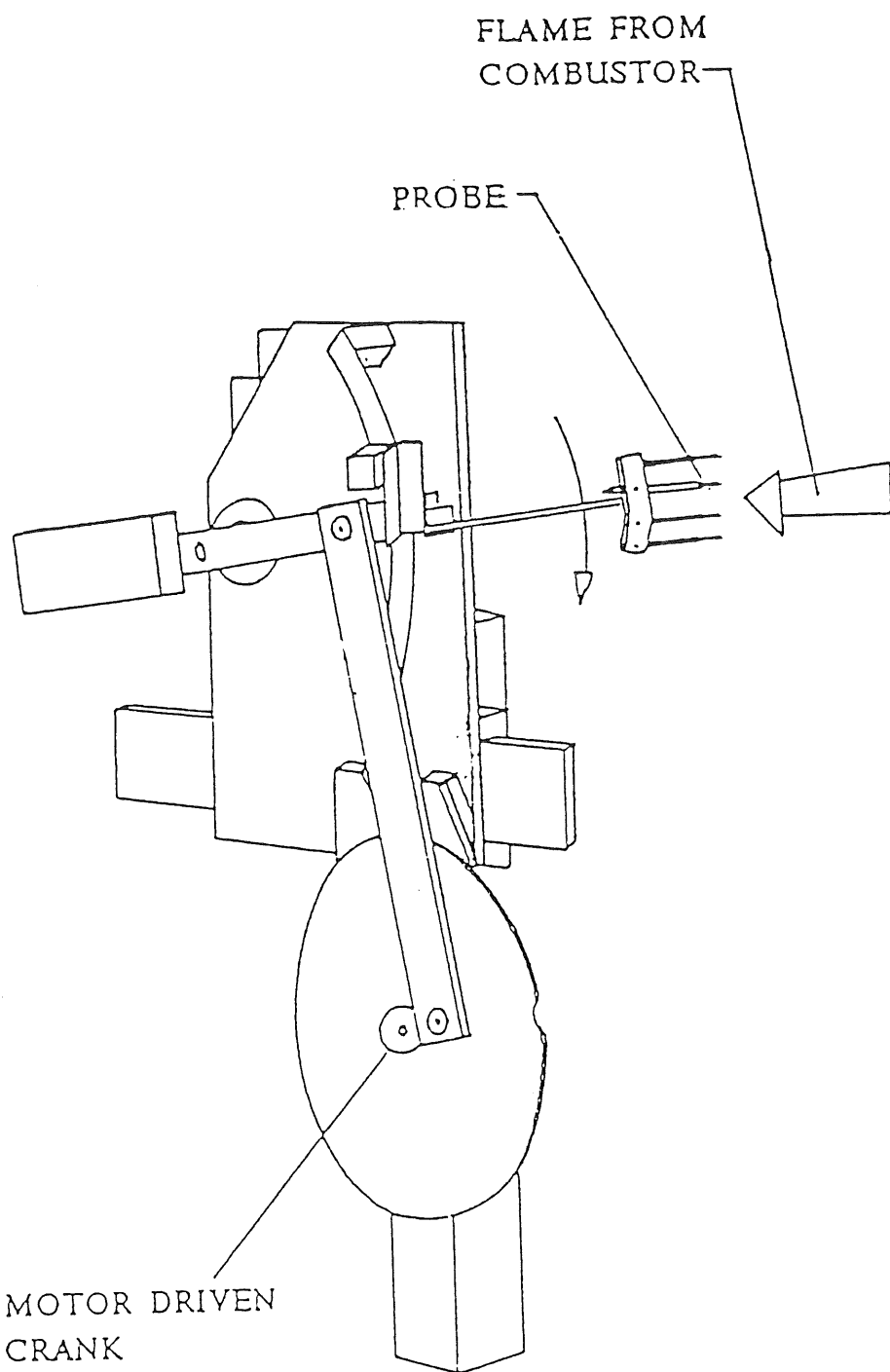


Figure 7
Fast Injection mechanism used by Moss&Oldfield (1991).
In flame residency time < 100 milliseconds.
Total transient injection process = 2 seconds (approximately).

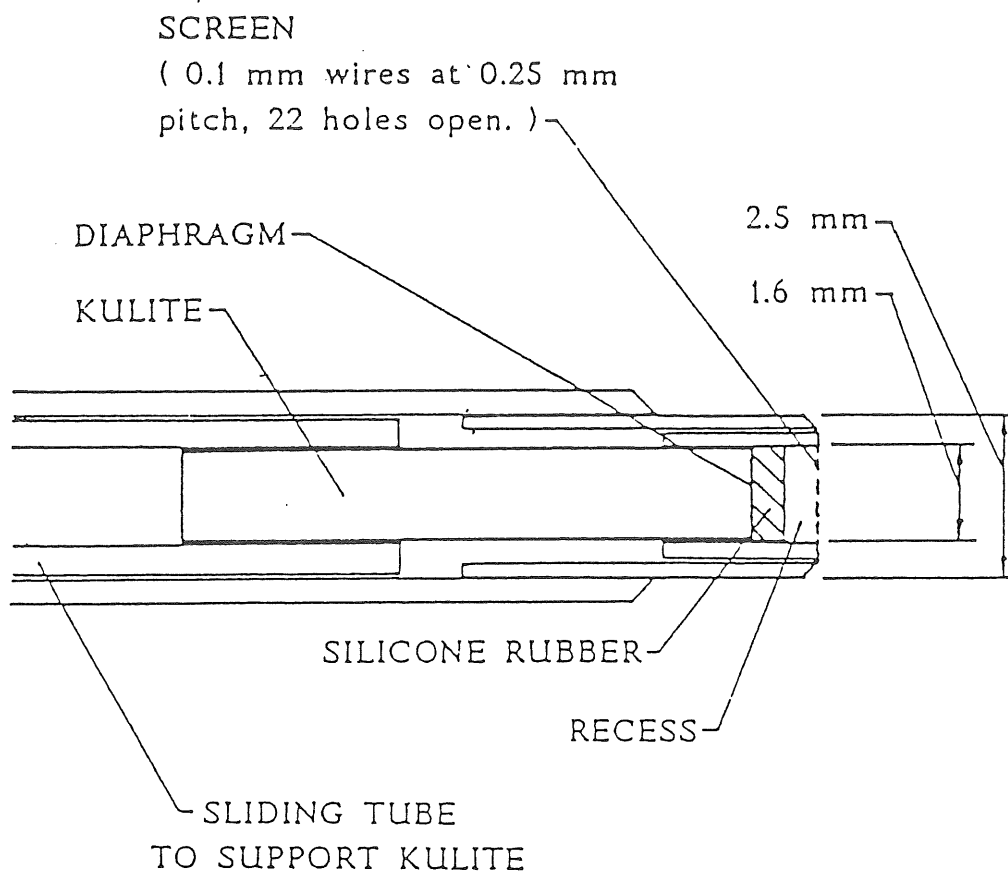


Figure 8
Turbulence intensity measurement device
made of a dynamic pressure transducer , Moss&Oldfield (1991).

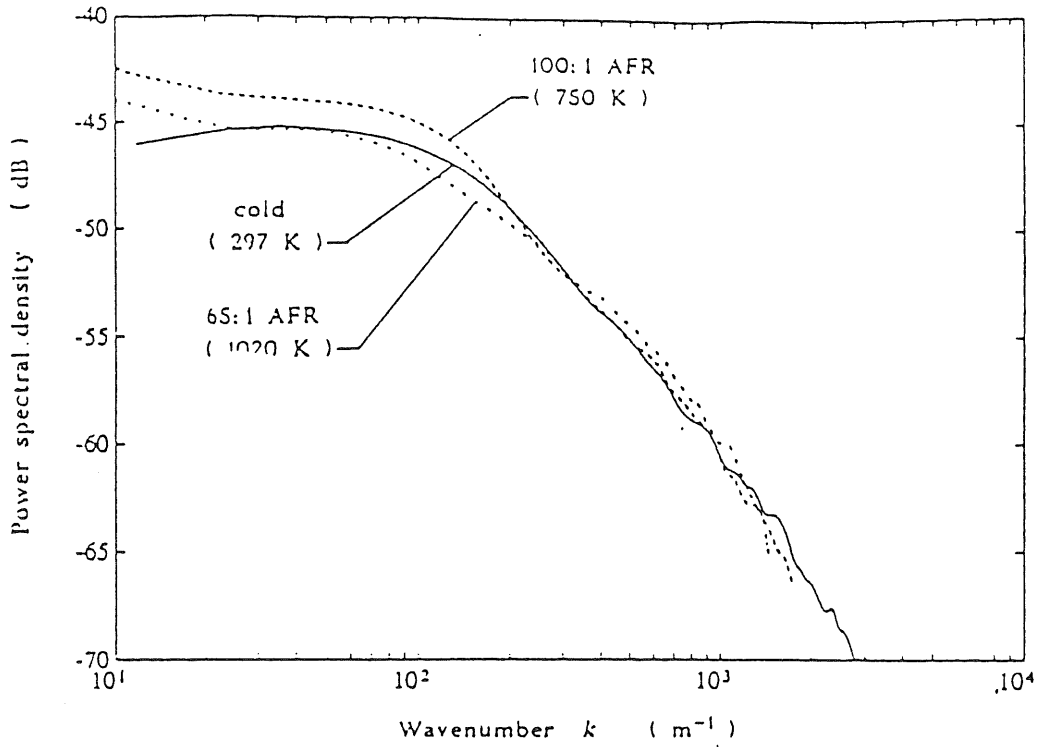


Figure 9

Turbulence wave number spectra, Combustor A , Moss&Oldfield (1991).
Cold test and two hot tests at different air-fuel ratios.

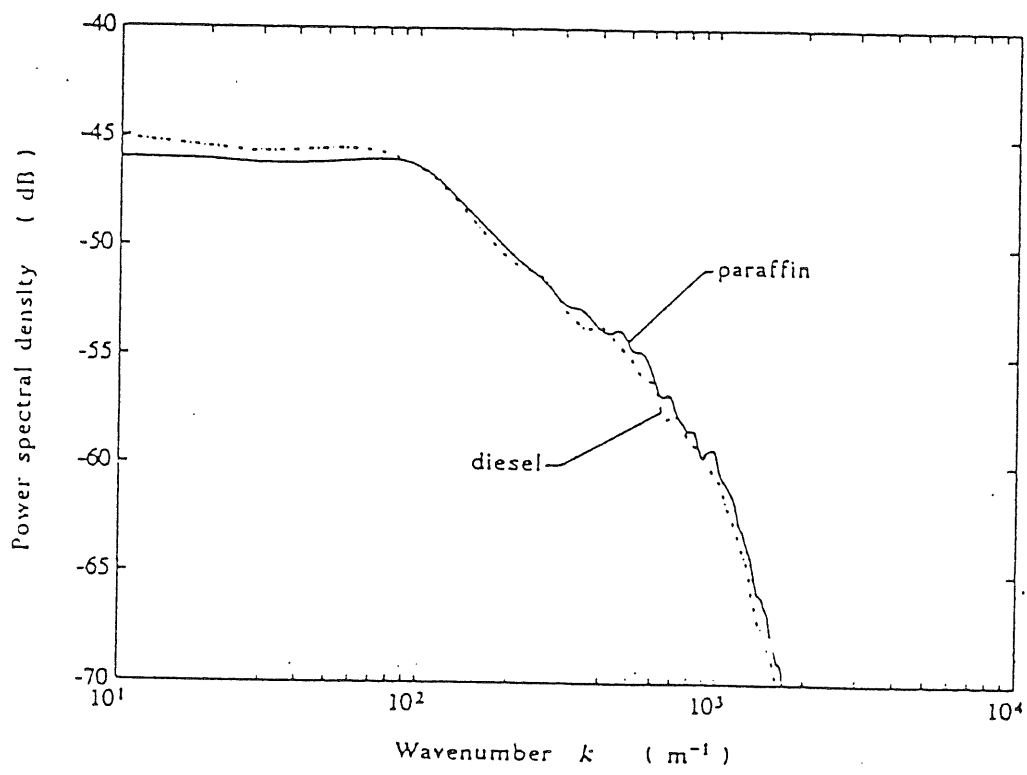


Figure 10

Influence of the type of the fuel on turbulence spectra, combustor B, Moss&Oldfield (1991)
Fuels : paraffin and diesel , air-fuel ratio 65:1

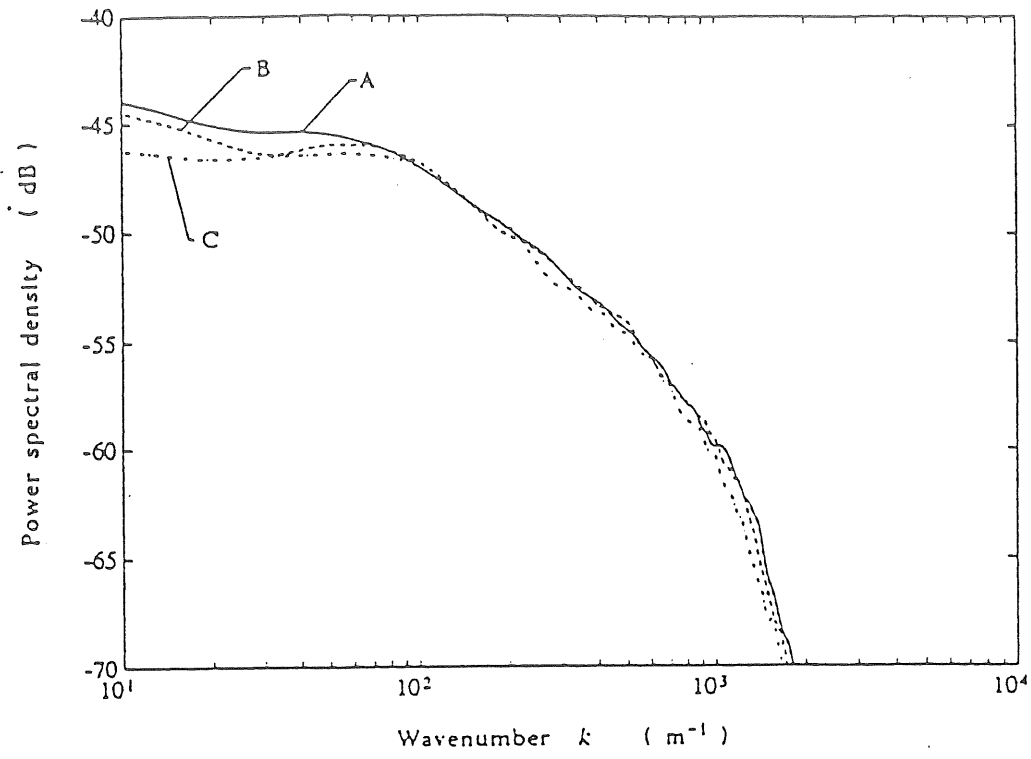


Figure 11

Comparison of turbulence spectra from three different combustors, Moss&Oldfield (1991).

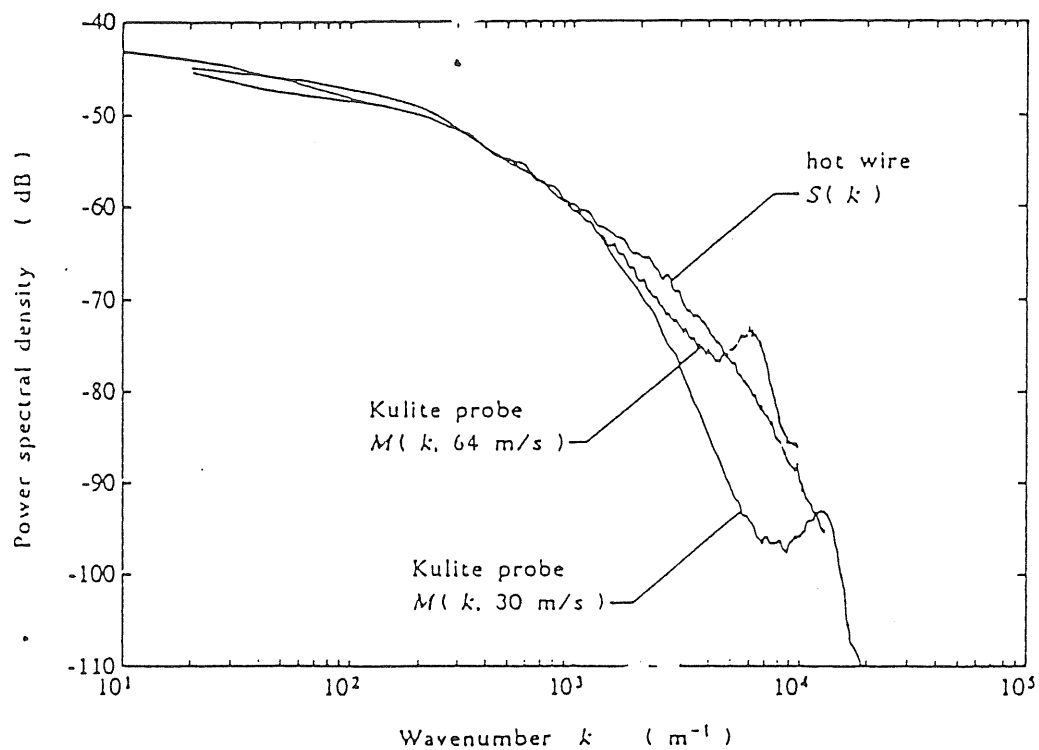


Figure 12

Calibration of the turbulence probe based on a dynamic pressure transducer.
Calibration in wind tunnel grid turbulence with hot wire , Moss&Oldfield (1991).

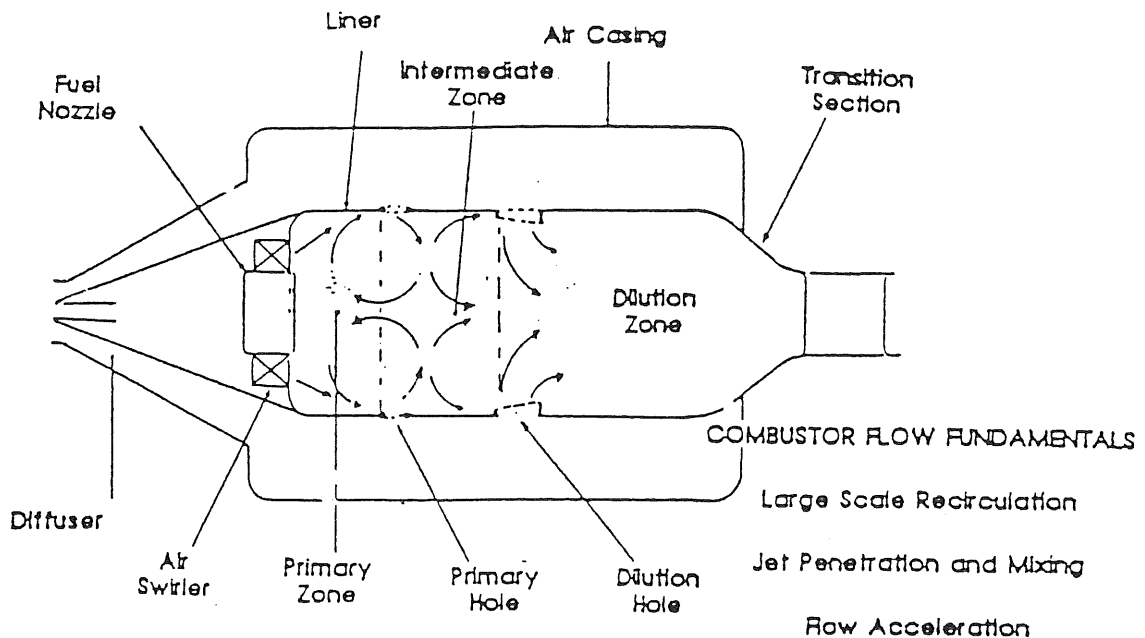


Figure 13
Description of combustor flow fundamentals , Ames&Moffat (1990)

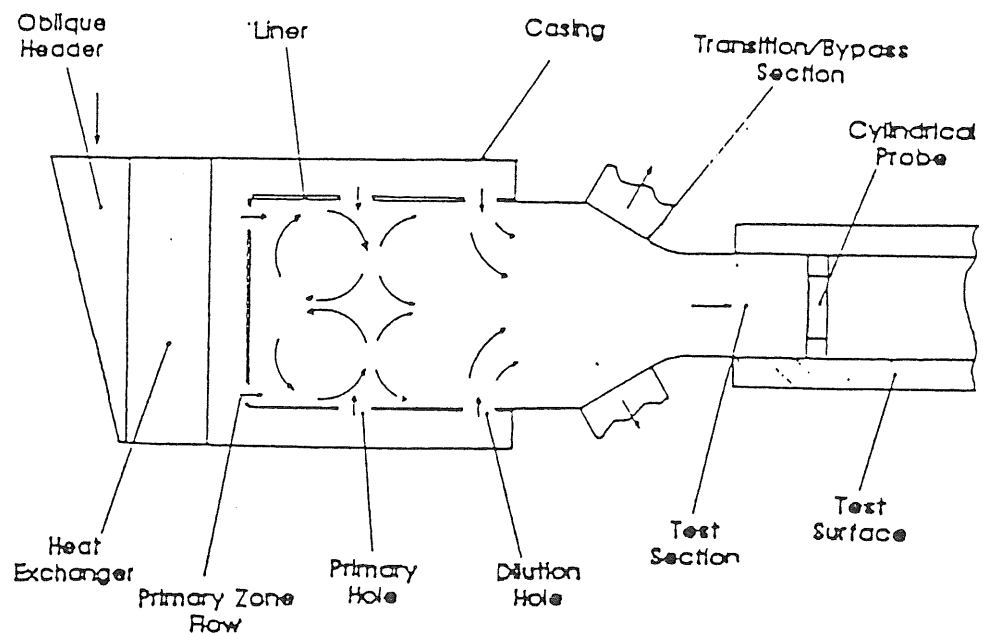


Figure 14
Schematic of the turbulence generator , Ames&Moffat (1990)

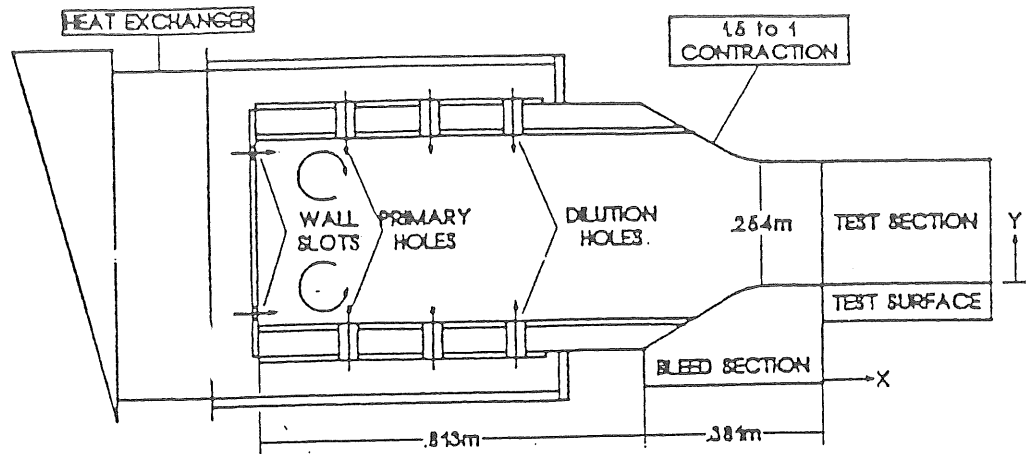


Figure 15
Details of the Turbulence generator , Ames&Moffat (1990)

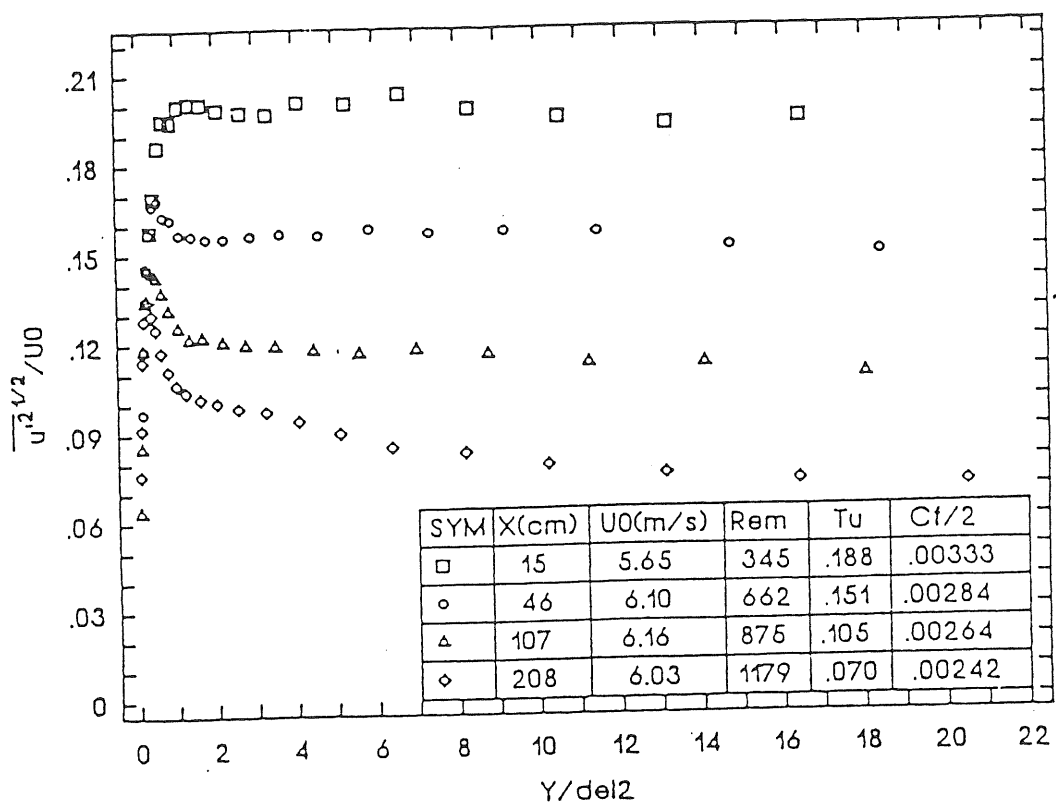


Figure 16
Streamwise turbulence intensity at different axial positions downstream of the combustor simulator , Ames&Moffat (1990)

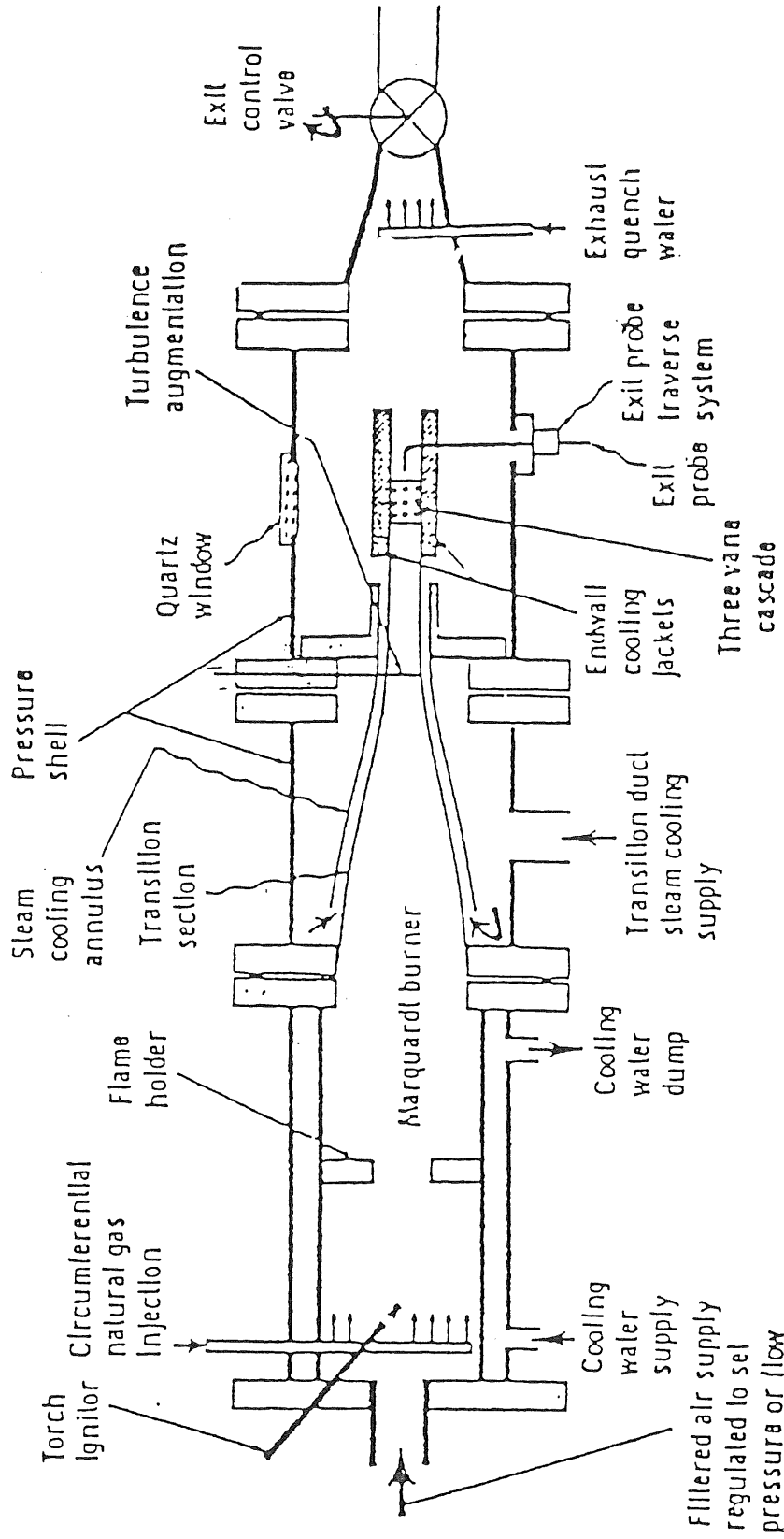


Figure 17
 A hot cascade facility with a Marquardt burner, (no dilution jets exist).
 York, Hylton and Mihalec (1984).

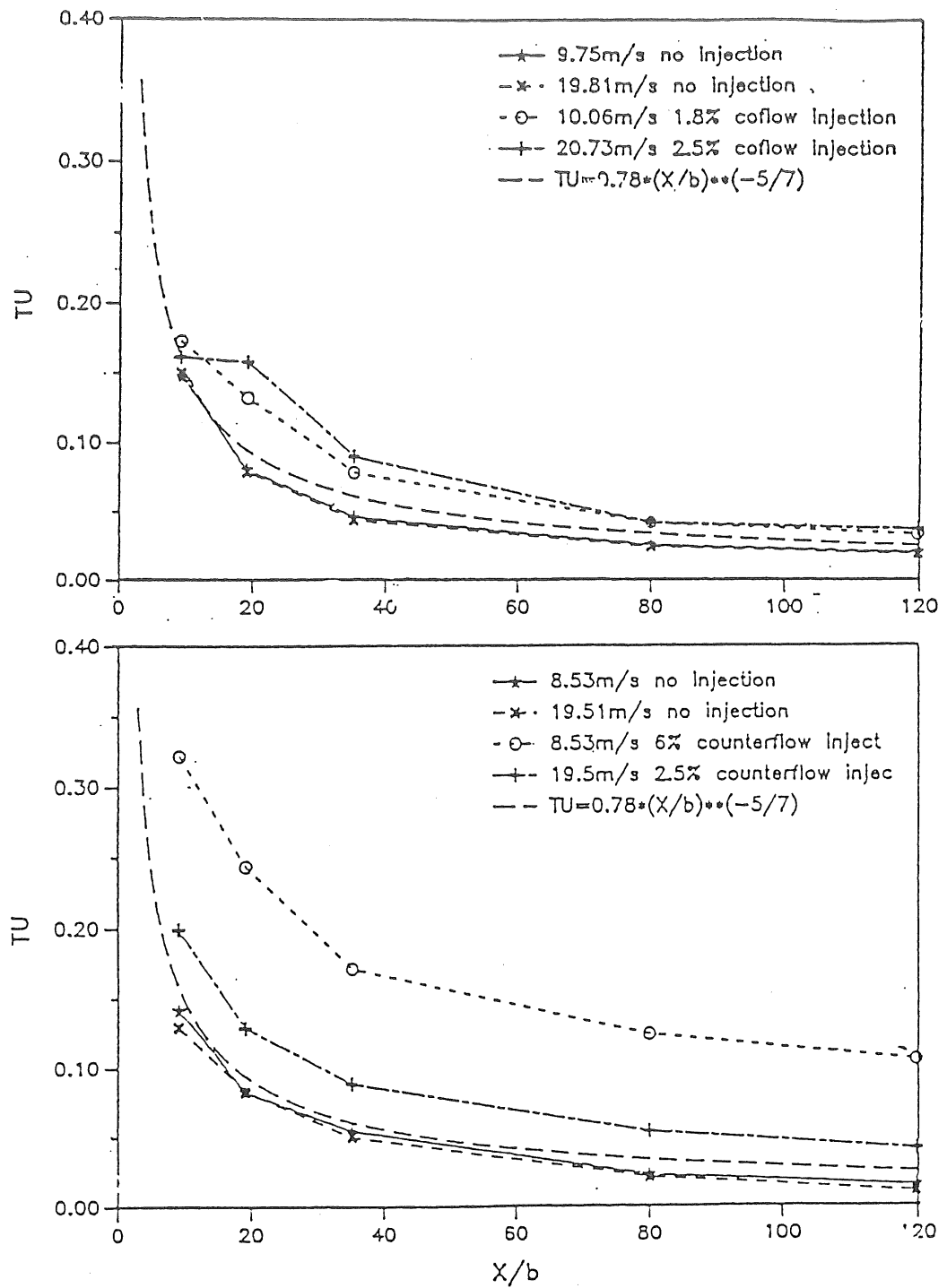


Figure 20
Streamwise decay of turbulence in the jet grid, Young&Han (1988).

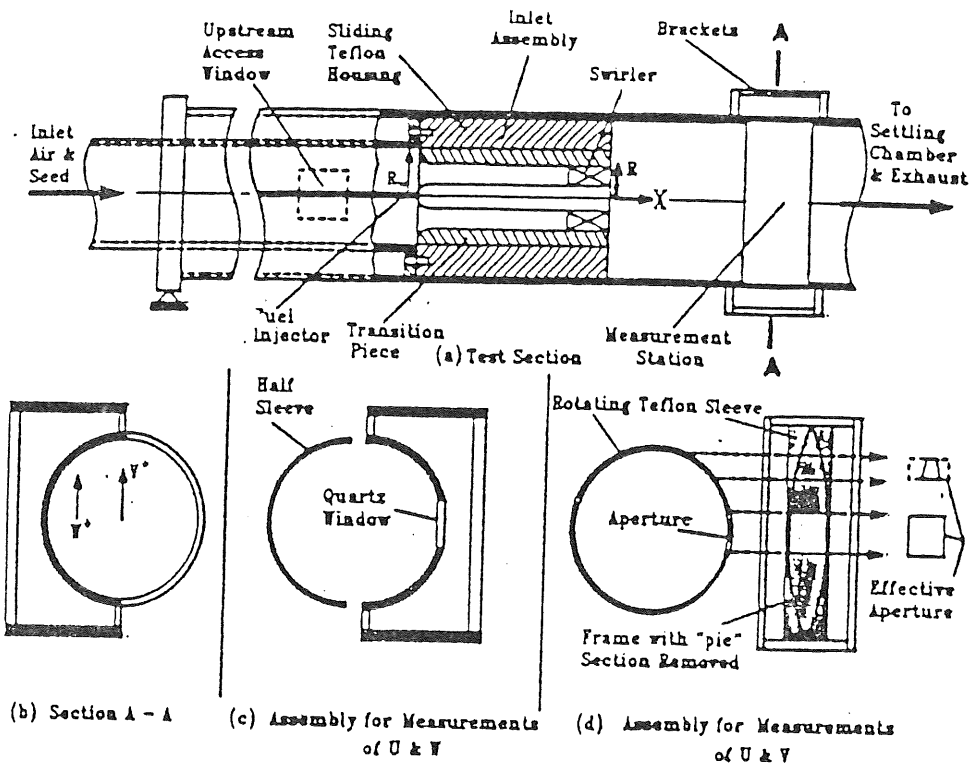


Figure 18
Swirling combustor with no dilution jets, Ahmed et al. (1992).

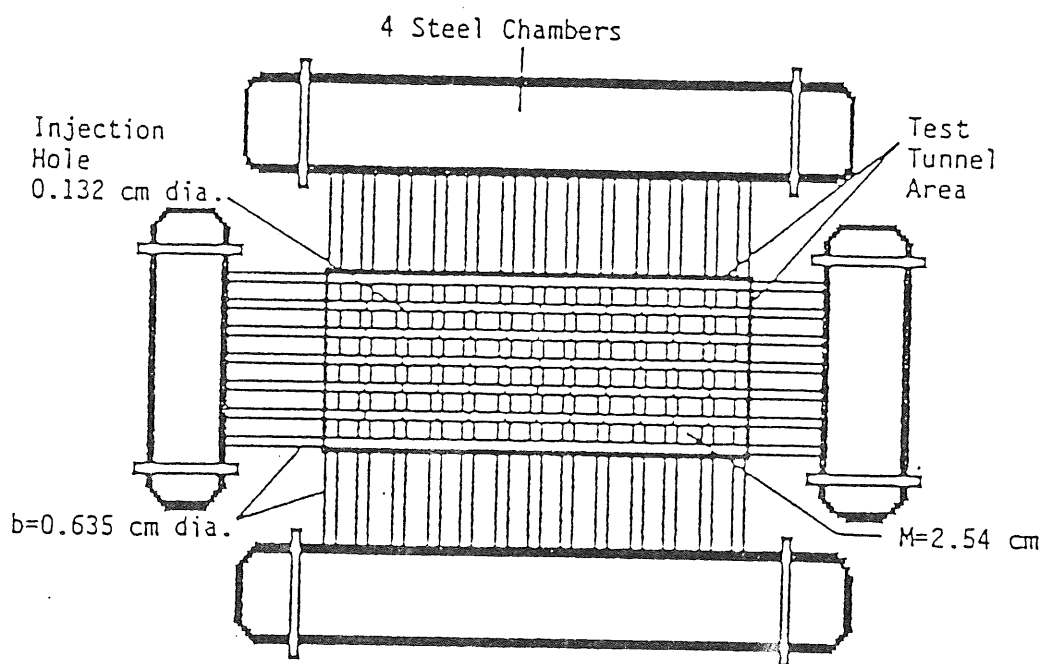
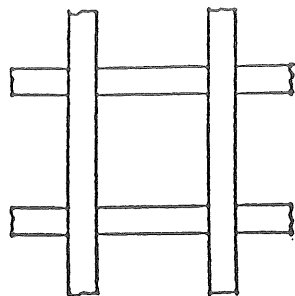
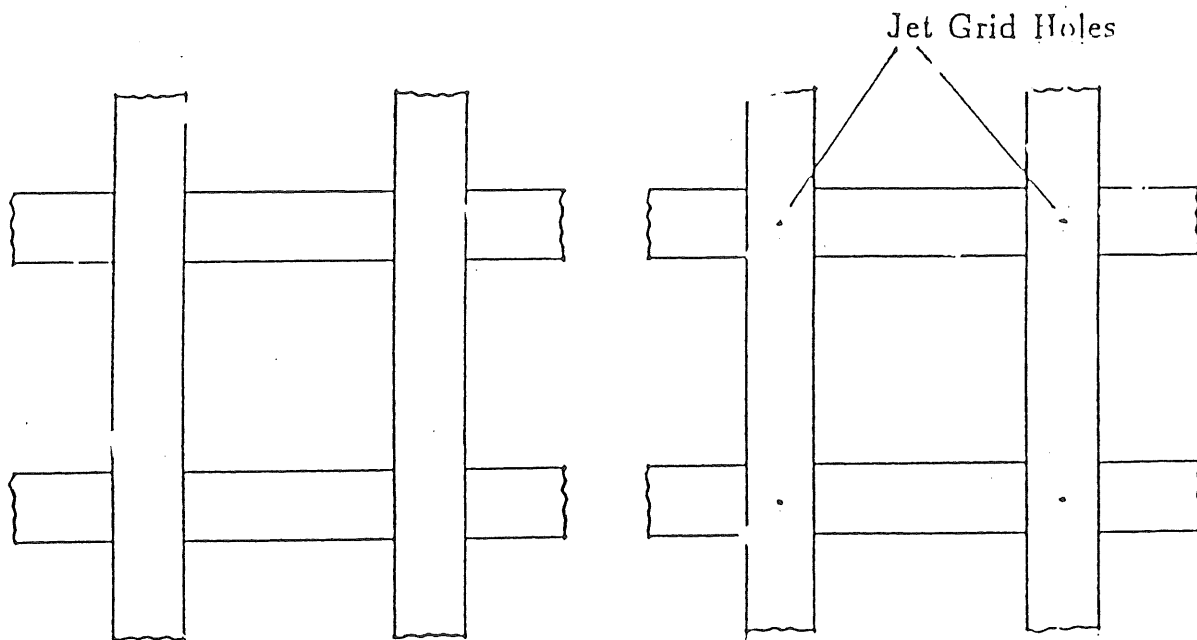


Figure 19
A jet grid type turbulence generator, Young&Han (1988).



Re _D	No Grid	Bar Grid	Passive Grid	Jet Grid
100,000	0.75	5.07	9.67	12.9
40,000	0.73	4.66	7.59	15.2
25,000	1.37	3.31	8.53	—

Bar Grid



Passive Grid

Jet Grid

Figure 21
A schematic of active passive/grids used by Mehendale et al. (1990)

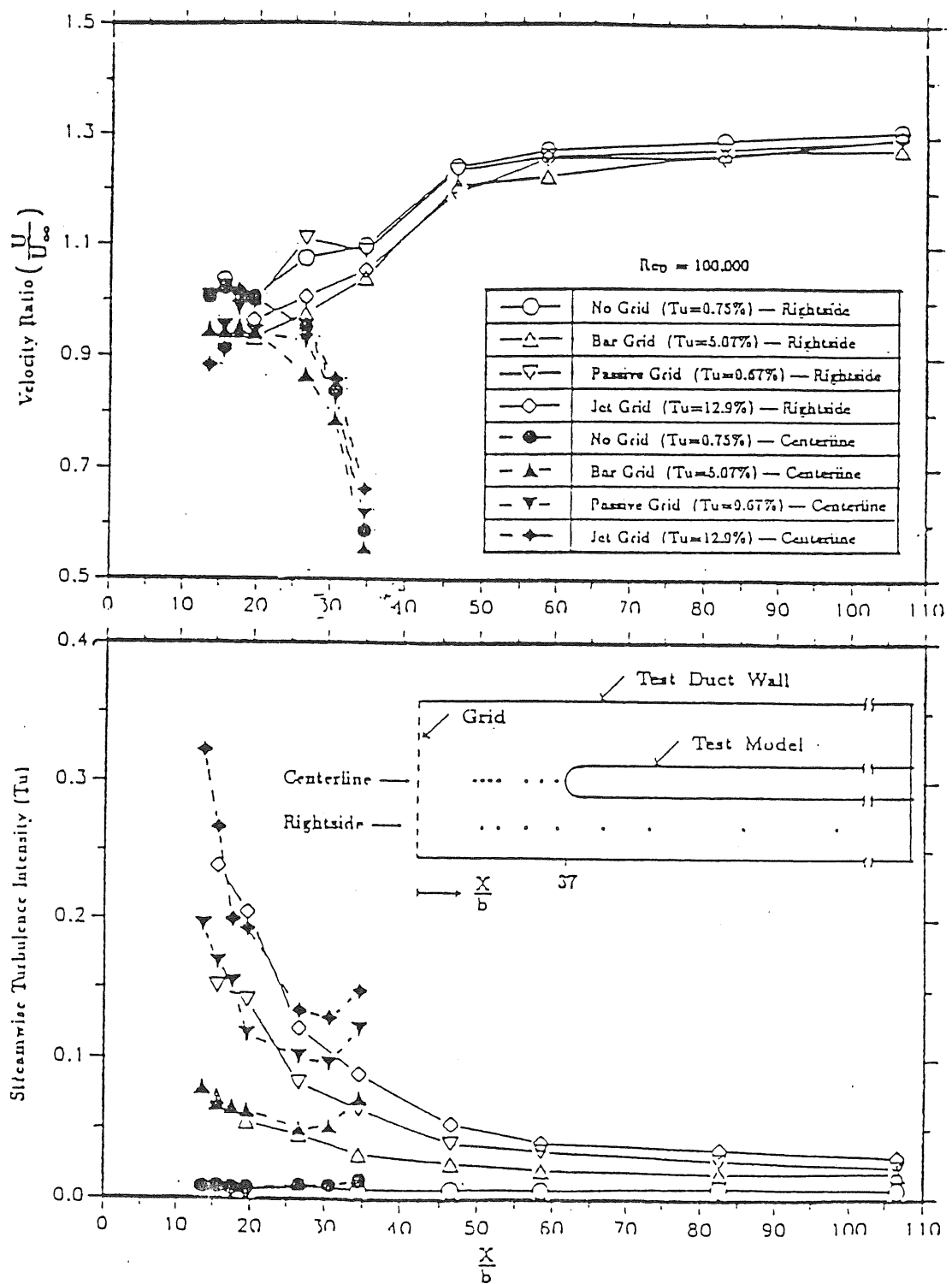


Figure 22
Streamwise distribution of normalized mainstream velocity and turbulence intensity,
Mehendale et al. (1990).

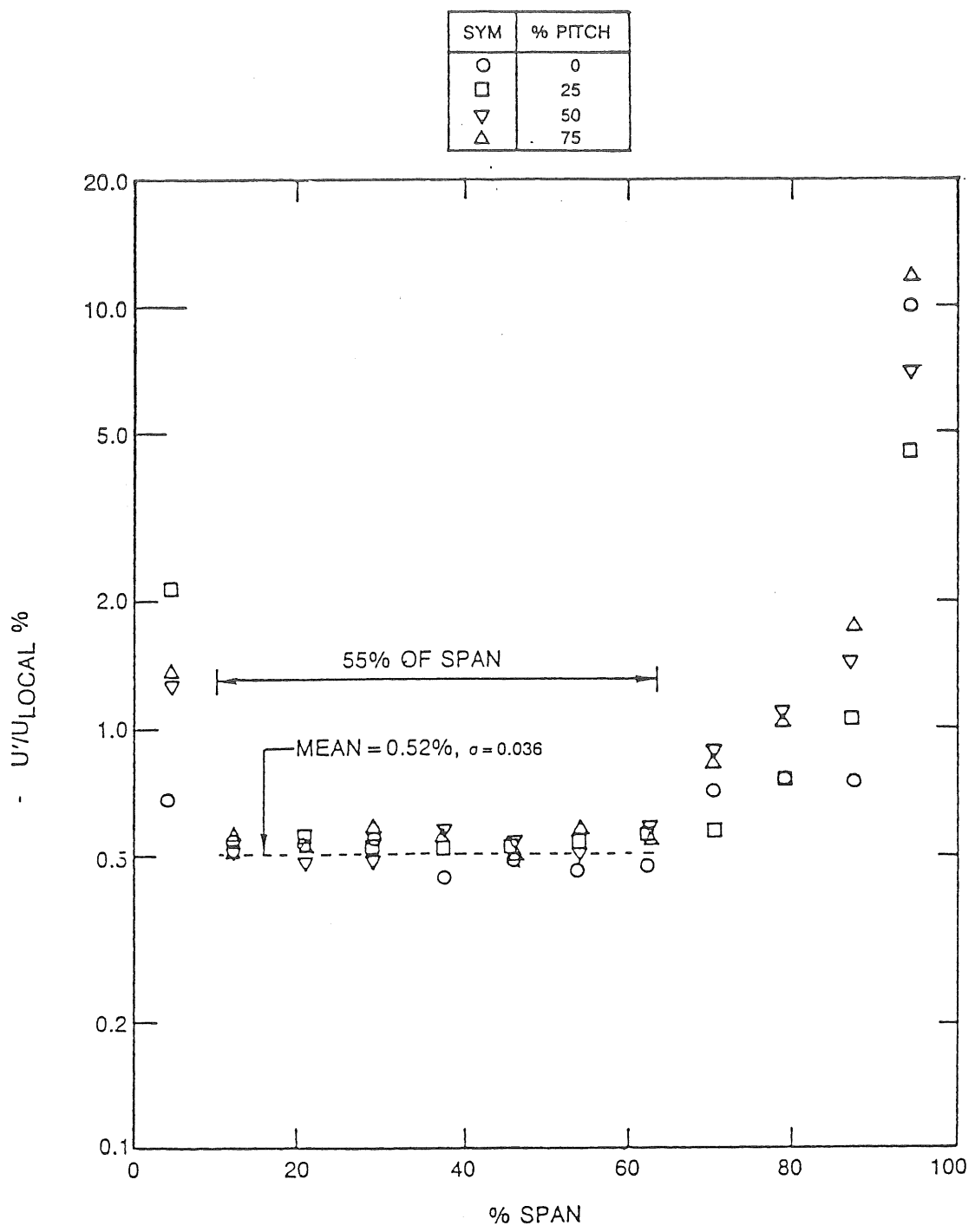


Figure 26
Streamwise turbulence intensity at 6.5 mesh length downstream distance from the grid,
Dring et al. (1986).

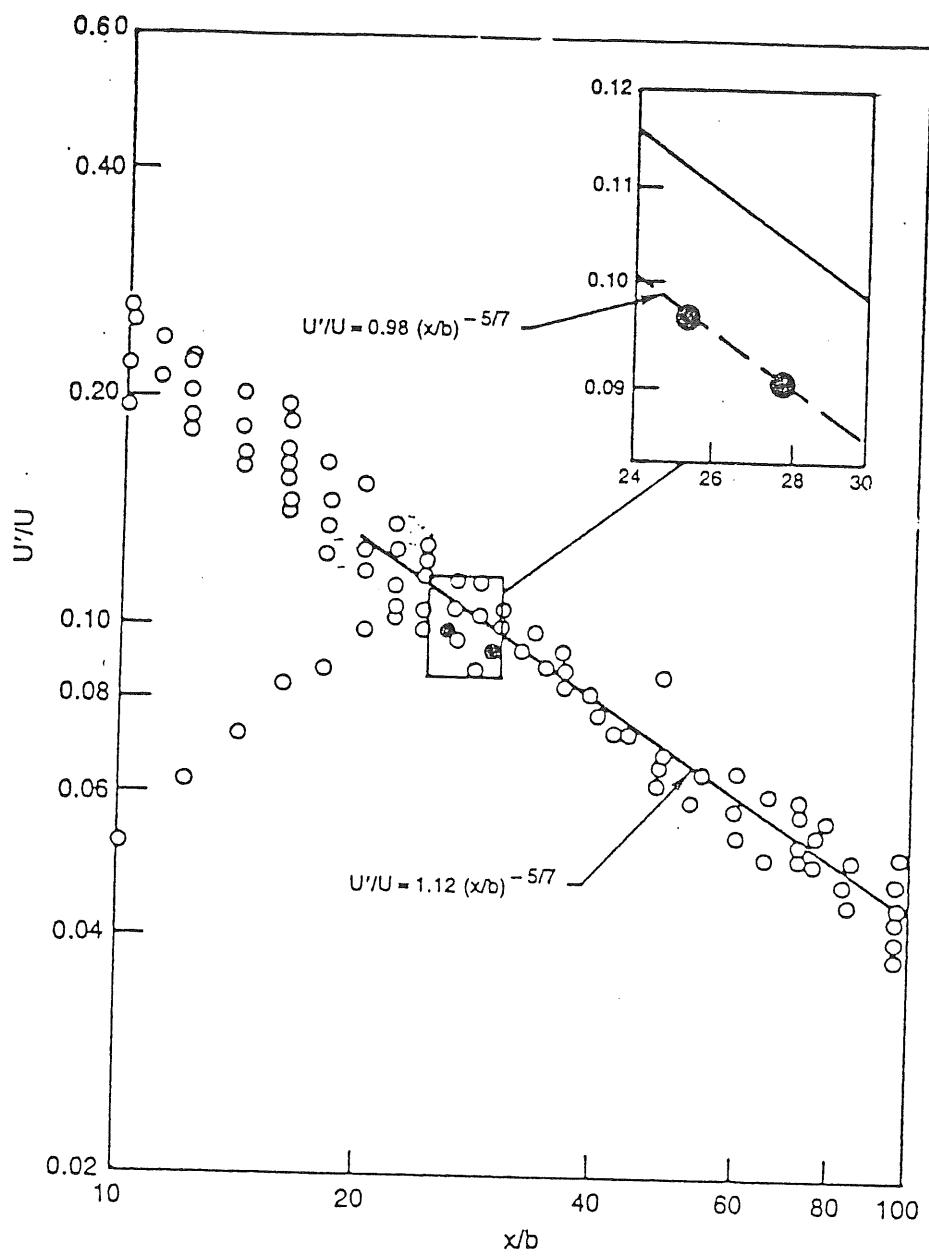


Figure 27
Decay of mid-span turbulence intensity and
comparison with bi-plane grid data of Baines and Peterson,
Dring et al. (1986).

APPENDIX - A

COMPUTER PROGRAM FOR CALCULATING HOT
CASCADE TOTAL PRESSURE
FOR A PRESCRIBED CASCADE TOTAL TEMPERATURE

A.FOR

A.DAT
CARRIES ENGINE DATA.

CURRENTLY MARS ENGINE CONDITIONS ARE IN THIS FILE.

HOWEVER A NEW ENGINE CONFIGURATION CAN BE INTERACTIVELY INPUT
INTO THE FILE FOR FUTURE USE.

C
C 7-23-1992 , CENGIZ CAMCI , SOLAR TURBINES INC.
C

C this program calculates HOT CASCADE operating conditions
C this version of the program uses MARS engine conditions
C as actual operating points.
C

C PRESCRIBED CASCADE TOTAL TEMPERATURE VERSION
C

C HOT CASCADE fluid is the same as the actual MARS engine
C The operating fluid is the combustion products of
C Natural gas/air mixture
C

C HOT GAS PROPERTIES ARE CALCULATED FROM A NASA HYDROCARBON TABLE
C SUBROUTINE "PROPGAS" INTERPOLATES FROM DISCRETE PROPERTY VALUES
C FOR THE SPECIFIC HEAT, GAMMA, ABSOLUTE VISCOSITY AND MOLECULAR
C PRANDTL NUMBER
C

C the HOT CASCADE geometry (gas side flow path) is the same as
C the MARS engine, however the total pressure and temperature
C in the hot cascade will be adjusted in such a way that
C

C Reynolds number
C AND
C Mach number
C

C WILL BE THE SAME FOR BOTH THE MARS ENGINE AND THE HOT CASCADE FLOW
C REYNOLDS NUMBER AND MACH NUMBER ARE CALCULATED AT THE BLADE EXIT
C FOR BOTH THE ENGINE AND THE HOT CASCADE
C

C SINCE THE TOTAL TEMPERATURE IS PRESENTLY "IMPOSED",
C FOR COOLED BLADE TESTS
C MAXIMUM ATTENTION SHOULD BE EXERCISED TO OBTAIN A REALISTIC
C COOLANT TO FREE STREAM TEMPERATURE RATIO
C

C The specific turbine passage is the first stage rotor
C

C REAL MTURB,MA2,M,MFR,MCMO,mcflux,mcool,MCOOLC
C

2222 WRITE(6,2222)

FORMAT(15X,'=====//
* 15x,'HOT CASCADE FACILITY FLOW/HEAT TRANSFER SIMULATION'//
* 15x,'SOLAR TURBINES INC. SAN DIEGO JUNE 1992'//
* 15x,'actual engine : MARS'//
* 15x,'CONFIGURATION : First stage rotor'//
* 15x,'prepared by : Cengiz Camci'//
* 15x,'=====//
*,/)

C READ THE CURRENT ENGINE DATA FOR HOT CASCADE SCALING
C CURRENT ENGINE : MARS FIRST STAGE AS OF 23-JULY-1992
C TURBINE ROTOR EXIT

```

      OPEN (UNIT=9,FILE='A.DAT',status='old')
      READ (9,555) CHORD,VREL2,PS2,TS2,MTURB,AREA,BETA,
*     BLNUM,chn,exarea,dhd,tcool,deltoc,mcmo
555   FORMAT(F11.0)
      close(9)
      write(6,6666) chord,vrel2,ps2,ts2,mturb,area,beta,
*     BLNUM,chn,exarea,dhd,tcool,deltoc,mcmo
6666   format(3x,'The current engine data before scaling'/
*           3x,'-----'/
*           3x,'CHORD LENGTH          [ INCHES ]',F8.3/
*           3X,'RELATIVE VELOCITY (ROTOR EXIT) [ FT/S ]',F8.1/
*           3X,'STATIC PRESSURE    (ROTOR EXIT) [ PSIA ]',F8.1/
*           3X,'STATIC TEMPERATURE (ROTOR EXIT) [ F ]',F8.1/
*           3X,'TURBINE MASS FLOW RATE [ LBM/S ]',F8.1/
*           3X,'ANNULAR FLOW AREA   [ INCH2 ]',F8.1/
*           3X,'EXIT FLOW ANGLE      [ DEG. ]',F8.1/
*           3X,'NUMBER OF BLADES           ',F8.1/
*           3x,'-----'/
*           3x,'number of coolant holes per blade      ',F8.1/
*           3x,'exit area per coolant hole   [ inch2 ]',F9.6/
*           3X,'hyd. diam. of the coolant hole [ inch ]',f9.6/
*           3x,'coolant temperature (blade root) [ deg.F ]',F8.1/
*           3x,'coolant temperature rise       [ deg.F ]',F8.1/
*           3x,'coolant to free stream mass f.r. ratio ',F8.5/
*           3X,'-----') )
3333   WRITE(6,4444)
4444   FORMAT(3X,'PRESS      "RETURN" if you dont need any change      '//'
*           3X,'PRESS      "123"      if you need to CHANGE ENGINE DATA',$/'
*           /3X,'-----')
      READ(5,666,ERR=3333) IFLAG
666   FORMAT(I3)
      IF(IFLAG.EQ.0) GO TO 9999
      IF(IFLAG.NE.123) GO TO 3333
C
      WRITE(6,1)
1     FORMAT(3X,'ENTER AVAILABLE DATA FROM ACTUAL CONFIGURATION'/
*           3X,'=====') //)
      WRITE(6,18)
C
C
18   FORMAT(3X,'ENTER CHORD LENGTH          CHORD [ IN. ] = ',$/)
      read(5,12) CHORD
12   format(f10.0)
C
      CONVERT CHORD LENGTH TO METER
      CHORD=CHORD*2.54E-2
C
      write(6,11)
11   format(3x,'RELATIVE VEL. AT THE EXIT      VREL2 [FT/S.] = ',$/)
      READ(5,12) VREL2
C
      CONVERT TO M/S
      VREL2=VREL2*.3048
      WRITE(6,13)
13   FORMAT(3X,'STATIC PRESSURE AT THE EXIT      PS2 [ PSIA ] = ',$/)
      READ(5,12) PS2
C
      CONVERT TO PA

```

```

PS2=PS2*6894.8
WRITE(6,14)
14 FORMAT(3X,' STATIC TEMPERATURE AT THE EXIT   TS2 [ F ] = ',$)
READ(5,12) TS2
C CONVERT TO K
TS2=(TS2+459.67)/1.8
WRITE(6,15)
15 FORMAT(3X,' TURBINE MASS FLOW RATE      MTURB      [LBM/S] = ',$)
READ(5,12) MTURB
C CONVERT TO KG/S
MTURB=MTURB*.45359
WRITE(6,16)
16 FORMAT(3X,' ANNULAR FLOW AREA AT THE EXIT          [INCH2] = ',$)
READ(5,12) AREA
C CONVERT TO M2
AREA=AREA*6.45E-04
WRITE(6,17)
17 FORMAT(3X,' BETA ANGLE FOR THROAT AREA           [DEG. ] = ',$)
READ(5,12) BETA
C
WRITE(6,177)
177 FORMAT(3X,' number of blades in the engine        = ',$)
READ(5,12) BLNUM
write(6,178)
178 format(3x,' number of coolant holes per blade     = ',$)
read(5,12) chn
write(6,179)
179 format(3x,' exit area per coolant hole          = ',$)
read(5,12) exarea
write(6,159)
159 format(3x,' coolant hole hydraulic diameter      [inch] = ',$)
read(5,12) dhd
write(6,181)
181 format(3x,' coolant temperature at the blade root [F] = ',$)
read(5,12) tcool
write(6,182)
182 format(3x,' engine coolant temperature rise         [F] = ',$)
read(5,12) deltoc
write(6,183)
183 format(3x,' coolant to free stream mass fl.rate ratio = ',$)
read(5,12) mcmo
open(unit=9,file='a.dat',status='old')
WRITE(9,5556) (CHORD/.0254), (VREL2/.3048), (PS2/6894.8),
* (TS2*1.8-459.67), (MTURB/.45359), (AREA/6.45E-04), beta, BLNUM,
* chn, exarea, tcool, deltoc
5556 format(f11.6)
GO TO 7777
9999 CONTINUE
C UNIT CONVERSIONS
CHORD=CHORD*0.0254
VREL2=VREL2*0.3048
PS2=PS2*6894.8
TS2=(TS2+459.67)/1.8
MTURB=MTURB*.45359
AREA=AREA*6.45E-4

```

```

C
7777    CONTINUE
C
C      CALCULATE EXIT RELATIVE MACH NUMBER
C
C      TX=TS2
C      CONVERT TS2 FROM K TO RANKINE FOR PROPGAS
C      TX=TX*1.8
C      TX IS IN RANKINE NOW
C
C      CALL PROPGAS(TX,VISX,CPX,GAX,PRX,RX)
C
C      GAMMA IS NON-DIMENSIONAL, NO NEED FOR CONVERSION
C      GA=GAX
C
C      PROPGAS RETURNS R IN SI (J/KG*K)
C      R=RX
C
C      SPECIFIC HEAT IS RETURNED BY PROPGAS AS (BTU/LB*R)
C      CONVERT SPECIFIC HEAT TO (J/KG*K)
C      1 BTU/(LB*R) = 4.184 KJ/(KG*K)
C      CPX=CPX*4.184
C      CP IS NOW IN KJ/(KG*K)
C      CP=CPX*1000.
C      CP IS NOW IN J/(KG*K)
C
C      PROPGAS RETURNS VISCOSITY AS LB/(FT*HR)
C      A CONVERSION TO Ns/M2 IS NEEDED AT THIS POINT
C      VISX=VISX*4.133789E-4
C
C      MA2=VREL2/SQRT(GA*R*TS2)
C      CALCULATE TURBINE EXIT DENSITY ROS2 [KG/M3]
C      ROS2=PS2/(R*TS2)
C      CALCULATE REYNOLDS NUMBER AT THE TURBINE EXIT
C      ABSOLUTE VISCOSITY AT TS2
C
C*****
VMARS=VISX
RE2= VREL2*ROS2*CHORD/VMARS
WRITE(6,40) MA2
40 FORMAT(3X,'ISENTROPIC MACH NUMBER AT THE TURBINE EXIT = ',F5.3)
WRITE(6,41) RE2
41 FORMAT(3X,'CHORD REYNOLDS NUMBER AT THE TURBINE EXIT = ',F8.0)
C
C      WRITE(6,23) ROS2,VMARS
C23   FORMAT(3X,'TURBINE EXIT STATIC DENSITY      [KG/M3] ',F10.3/
C      *      3X,'TURBINE EXIT VISCOSITY          [Ns/M2] ',E10.5/
C      *      3X,'-----' /)
C
C      CALCULATE RELATIVE TOTAL TEMPERATURE AT TURBINE ROTOR EXIT
C      NOTE THAT RELATIVE STAGNATION ENTHALPY IS CONSERVED IN A TURBINE ROTOR
TREL2=(CP*TS2+0.5*VREL2*VREL2)/CP
C      EFFECTIVE TOTAL GAS TEMPERATURE FOR ROTOR HEAT TRANSFER TGAS [K]
C      FACTOR TAKES CARE OF THE RADIAL TEMPERATURE DISTRIBUTION
C      FOR FURTHER DETAILS SEE THE WRITE-UP BY DAVE EVANS (PAGE 52)

```

FACTOR=1.05
TGAS=TREL2*FACTOR

THIS SECTION TAKES CARE OF MACH NUMBER SIMILARITY
CALCULATE TOTAL TO STATIC PRESSURE RATIO (TURBINE)
CORRESPONDING TO MA2
A=GA/ (GA-1)
B= (GA-1.) /2.
PR=(1+B*MA2*MA2) **A
CALCULATE TOTAL TO STATIC TEMPERATURE RATIO (TURBINE)
CORRESPONDING TO MA2
TR=(1+B*MA2*MA2)

ACTUAL MASS FLUX RATE OF THE TURBINE
RWACT=ROS2 *VREL2
STATIC PRESSURE DIVIDED BY SQRT (STATIC TEMPERATURE)
PSQRT=RWACT / (MA2*SQRT (GA/R))

6789 CONTINUE
NOW ENTER THE STAGNATION TEMPERATURE YOU WANT TO GENERATE
IN THE HOT CASCADE TEST SECTION
WRITE(6,20)
FORMAT(3X,'ENTER THE PRESCRIBED STAGNATION TEMPERATURE [F] ',\\$)
READ(5,12) TOCASC
IF(TOCASC.EQ.0) STOP
CONVERT TO K
TOCASC=(TOCASC+459.67)/1.8

CALCULATE HOT CASCADE STATIC TEMPERATURE
NOTE THAT HC DENOTES HOT CASCADE CONDITIONS

FIRST PASS FIRST PASS FIRST PASS
FLUID PROPERTIES IS AT MARS STATIC CONDITIONS
ISWITCH=0 INDICATES THE FIRST PASS
ISWITCH=0
TSHC=TOCASC/TR
IF (ISWITCH.EQ.1) SECOND PASS SECOND PASS
STATIC TEMPERATURE IN THE CASCADE IS CALCULATED
WITH FLUID PROPERTIES EVALUATED AT
(CLOSE TO REAL) HOT CASCADE ST. TEMP.

33333 CONTINUE
IF(ISWITCH.EQ.1) TSHC=TOCASC/CC
IF(ISWITCH.EQ.1) ISWITCH=ISWITCH+1
CONVERT TSHC FOR PROPGAS COMPATIBILITY, CONVERT FROM K TO R
Tx=TSHC*1.8
CONVERT TO F
TXA=TX-459.67

1111 WRITE(6,4111) TXA
FORMAT(3X,'-----',/
* 3X,'STATIC TEMPERATURE IN THE HOT CASCADE [F] ',F6.1/
* 3X,'-----')

```

C
C
C     CALL PROPGAS(TX,VISX,CPX,GAX,PRX,RX)
C     CONVERT VISHC TO nS/M2
C     VISHC=VISX*4.133789E-4
C     VR=VISHC/Vmars
C     write(6,9777) vishc/4.133789E-4,1./vr
9777   *      FORMAT(3X,'VISCOSITY AT THE HOT CASCADE EXIT [LB/FT*HR] ',F11.4/
C             *      3X,'ENGINE TO CASCADE VISCOSITY RATIO ',F11.4)

C
C     CALCULATE THE REQUIRED HOT CASCADE STAGNATION PRESSURE
C     TO GENERATE THE RE AND Ma SIMULATION AT A PRESCRIBED HOT CASCADE
C     STAGNATION TEMPERATURE
C     VR = RATIO OF ABS. VISCOSITY IN THE (HOT CASCADE) TO (MARS ROTOR)
C
C     THE FOLLOWING EQUATION IS
C     ENCINE REYNOLDS NUMBER = HOT CASCADE REYNOLDS NUMBER
C     SEE THE WRITE UP *****
C
C     PO=VR*RWACT / (MA2*SQRT(GAX/RX))
C     CC=1.+ (GAX-1.)*MA2*MA2/2.
C     PO=PO*CC** (GAX/ (GAX-1.))
C     PO=PO*SQRT(TOCASC/CC)
C     iswitch=2 means the second pass is complete
C     fluid properties calculated at hot cascade
C     exit static conditions
C
C     IF(ISWITCH.EQ.2) GO TO 8888
C     ISWITCH=1
C
C     GO TO 33333
8888   CONTINUE
C
C     WRITE(6,30) CC** (GAX/ (GAX-1.))
C30    FORMAT(3X,'TOTAL TO STATIC PRESSURE RATIO FOR MA SIMILARITY =',F6.2)
C     WRITE(6,31) CC
C31    FORMAT(3X,'TOTAL TO STATIC TEMPERA. RATIO FOR MA SIMILARITY =',F6.2/)
C     TOCASC=TOCASC*1.8-459.67
C     WRITE(6,32) TOCASC
C32    FORMAT(3X,'*****//'
C             *      3X,'PRESCRIBED HOT CASCADE TOTAL TEMPERATURE IN F =',
C             *      F6.1/) .
C     WRITE(6,33) (PO/6894.8)
C33    FORMAT(3X,'CASCADE TOTAL PRESSURE SHOULD BE SET TO (PSIA) =',
C             *      F6.1//'
C             *      3X,'*****')
C
C     CALCULATE THE REQUIRED MASS FLOW RATE UNDER THE CURRENT
C     HOT CASCADE CONDITIONS
C
C     MASS FLUX RATE WAS ALREADY CALCULATED AS [RWACT]
C     TOTAL EFFECTIVE AREA OF THE HOT CASCADE IS DEFINED WITH THE NUMBER OF
C     CASCADE PASSAGES
C     FOR THE CURRENT PROGRAM THERE ARE 5 CASCADE BLADES (4 PASSAGES)
C     MARS ENGINE HAS 88 TURBINE ROTOR BLADES (88 PASSAGES)

```



```

* ' TEMPERATURE RATIO ',F8.3/
* 3X,'absolute temperature ratio at blade root' /)

C
C "TOCASCB" IS THE PRESCRIBED HOT CASCADE TOTAL TEMPERATURE IN F
C WE ARE KEEPING THE SAME COOLANT TO GAS (RELATIVE) TEMPERATURE
C RATIO OF THE ENGINE
C THE SAME VALUE WILL BE APPLIED TO HOT CASCADE OPERATION
C
C TCHC IS THE HOT CASCADE COOLANT TEMPERATURE
C AT THE blade root location
C TCHC=TCTO*(Tocasc+459.67)
C CONVERSION FROM R TO F
C TCHC=TCHC-459.67
C WRITE(6,345)TCHC
345   FORMAT(3X,'HOT CASCADE COOLANT TEMPERATURE AT THE',
*          ' BLADE ROOT      [ F ]      ',F8.1/)

C
C USE NON-DIMENSIONAL COOLANT TEMPERATURE RISE RELATION
C FROM THE ENGINE DATA TO ESTIMATE THE COOLANT INLET TEMPERATURE
C AT THE BLADE ROOT OF THE CASCADE BLADE
C
C DELHC=EPSILON*(TOCASCB-TCHC)
C
C ESTIMATE THE PASSAGE EXIT TEMPERATURE OF THE COOLANT IN [F]
C
C TCHCEX=TCHC+DELHC
C WRITE(6,7771) DELHC
7771  format(3x,'Estimated coolant temperature rise ',
*          'in the cascade      [ F ]      = ',F6.1)
        write(6,7666) tchcex
7666  format(3x,'Coolant temperature at the passage exit [F]',
*          15x,F10.1/)

C Reynolds number of the hot cascade coolant fluid at
C the coolant passage exit will be calculated by using TCHCEX
C mcmo = COOLANT TO FREESTREAM MASS FLOW RATE RATIO
C
C CALCULATE engine COOLANT MASS FLOW RATE (MCMO*mturb) in kg/sec
C
C mcool=mcmo*mturb
C calculate coolant mass flux rate kg/(m2*sec)
C mcflux=mcool/(blnum*chn*exarea*0.0254*0.0254)
C CALCULATE ABSOLUTE VISCOSITY AT THE COOLANT PASSAGE EXIT
C TURBINE
C TTC=TCOOL+DELOTOC+459.67
C CALL PROPGAS(TTC,VISENG,CPX,GAX,PRX,RX)
-----
C
C CALCULATE TURBINE COOLANT REYNOLDS NUMBER
C DEFINED AT THE PASSAGE EXIT
C RECOL=MCFLUX*DHD*.0254/(VISENG*4.133789E-4)
C
C write(6,8681) RECOL
8681  FORMAT(3X,'COOLANT REYNOLDS NUMBER (ENGINE)  /
*          3X,'BASED ON HYDRAULIC DIAMETER (EXIT) = ' ,F8.0)
C
C -----

```

CALCULATE THE COOLANT MASS FLUX RATE AT THE HOT CASCADE
TO MATCH THE COOLANT REYNOLDS NUMBER OF THE ENGINE
COOLANT TEMPERATURE AT THE CASCADE EXIT IN F TCHCEX
CONVERT TO R FOR THE PROPERTY TABLE
TCHCEX=TCHCEX+459.69

CALL PROPGAS(TCHCEX,VISCASC,CPX,GAX,PRX,RX)
COOLANT VISCOSITY RATIO (HOT CASCADE TO ENGINE)
VRATIO=VISCASC/VISENG

CASCADE COOLANT MASS FLUX RATE AT THE EXIT

COOLFLUX=MCFLUX*VISCA\$C/VISENG

CASCADE COOLANT MASS FLOW RATE IN KG/SEC

MCOOLC=COOLFUX*CHN*EXAREA*0 0254*0 0254

IN LBS/SEC.

MCOOT.C=MCOOT.C*2 2046

CASCADE COOLANT MASS FLOW RATE

SHARPE COOLANT FOR ONLY ONE BLADE

FOR ONE ONE BEADE
WHITE (6 3381) MCQOLC

```
FORMAT(3X,'CASCADE COOLANT MASS FLOW RATE',  
      3X,'FOR ONLY ONE BLADE [ LBS/SEC ] =',F7.4))
```

CONTINUE

STOP

END

APPENDIX - B

PROPGAS

A COMPUTER PROGRAM FOR THE GENERATION OF
PROPERTIES
OF NATURAL GAS/AIR COMBUSTION PRODUCTS

SUBROUTINE PROPGAS(TX,VISX,CPX,GAX,PRX,R)

THIS SUBROUTINE CALCULATES THE FLUID PROPERTIES
OF HYDROCARBON/AIR COMBUSTION PRODUCTS

PREPARED BY CENGIZ CAMCI
JUNE 1992
FOR SOLAR TURBINES INC. SAN DIEGO

SOURCE : THERMODYNAMIC AND TRANSPORT COMBUSTION PROPERTIES OF
HYDROCARBONS WITH AIR
NASA TECHNICAL PAPER 1908, 1982, PP: 145:147
SANFORD GORDON

fuel h/c atom ratio = 2.100
F/A=0.050248
CHEM. EQUIV. RATIO = 0.750
MOLECULAR WEIGHT=28.8596 KMOL
GASEOUS COMPOSITION
CO2=.09804 H2O=.10262 N2=.74077 O2=.04968 AR=.00888
universal gas constant 8314.34 J/[KMOL.K]
GAS CONSTANT 8314.34/28.8596
DIMENSION T(22),VIS(22),CP(22),GA(22),PR(22)

TEMPERATURE ARRAY IN RANKINE

DATA T/360., 460., 560., 660., 760., 860., 960., 1060.,
* 1160., 1260., 1360., 1460., 1560., 1660., 1760., 2100., 2600.,
* 3100., 3600., 4100., 4600., 5100./

CP ARRAY IN BTU/(LB*R)

DATA CP/.2478,.2493,.2514,.2540,.2571,.2604,.2640,.2678,.2717,
* .2757,.2796,.2835,.2872,.2908,.2942,.3039,.3153,.3239,
* .3303,.3350,.3386,.3413/

GAMMA ARRAY

DATA GA/1.3845,1.3812,1.3768,1.3715,1.3655,1.3591,1.3525,1.3457,
* 1.3391,1.3326,1.3264,1.3205,1.3151,1.3100,1.3054,1.2927,
* 1.2791,1.2697,1.2631,1.2585,1.2551,1.2525/

VISCOSITY ARRAY IN [LB/(FT*HR)]

DATA VIS/.0286,.0359,.0426,.0489,.0547,.0602,.0654,.0704,.0753,
* .0799,.0844,.0888,.0930,.0971,.1011,.1141,.1316,.1479,
* .1633,.1778,.1917,.2049/

PRANDTL NUMBER

DATA PR/.7730,.7562,.7508,.7506,.7481,.7477,.7472,.7457,.7436,
* .7413,.7392,.7373,.7359,.7348,.7338,.7315,.7293,.7262,
* .7226,.7195,.7160,.7119/

GAS CONSTANT FOR COMBUSTION PRODUCTS IN [(J/KG*K)]

CONVERSION [0.068596 (KJ/KG*K)=1 BTU/(LBM*R)]

R=UNIVERSAL GAS CONSTANT/[MOLECULAR WEIGHT]=8314.34/28.8596

R IN (J/KG*K) FOR THE COMBUSTION PRODUCTS OF AIR AND HYDROCARBON

R=288.096

IF(TX.LT.T(1).OR.TX.GT.T(22)) WRITE(6,9876)

IF(TX.LT.T(1).OR.TX.GT.T(22)) RETURN

FORMAT(3X,'*****WARNING *****',/
* 3X,'SPECIFIED TEMPERATURE IS OUT OF RANGE' /)

```
*      3X,' TEMPERATURE SHOULD BE EITHER GREATER THAN - 99 F' /
*      3X,' OR' /
*      3X,' TEMPERATURE SHOULD BE SMALLER THAN + 4640 F' /
*      3X,' *****')
DO 222 L=1,21
IF(TX.LT.T(L+1).AND.TX.GE.T(L)) GO TO 888
GO TO 222
888    CONTINUE
       TTT = (TX-T(L)) / (T(L+1)-T(L))
       CPX = ( CP(L+1) - CP(L) ) * TTT + CP(L)
       GAX = ( GA(L+1) - GA(L) ) * TTT + GA(L)
       VISX=(VIS(L+1)-VIS(L))*TTT+VIS(L)
       PRX = ( PR(L+1) - PR(L) ) * TTT + PR(L)
222    CONTINUE
RETURN
END
```

APPENDIX - C

A TABULATION FOR THE PROPERTIES OF NATURAL
GAS/AIR COMBUSTION PRODUCTS , GORDON (1982)

TABLE 14A - PROPERTIES BASED ON CONSTANT GASEOUS COMPOSITIONS

FUEL H/C ATOM RATIO = 2.100; DRY AIR:										F/A=0.050248; EQUIV. COMPOSITION: C02=.09804; H2O=.10262; N2=.74077; O2=.06968; AR=.0888							
T	(P=1.0)	DENSITY	H	(P=.01)	(P=.10)	ENTROPY (P=1.0)	(P=10.)	(P=50.)	CP	GAM	BTU/LB R	BTU/LB R	BTU/LB R	BTU/LB R	BTU/FT HR R	BTU/FT HR R	
R	LB/FT3	LB/LB	BTU/LB	BTU/LB	BTU/LB	BTU/LB	BTU/LB	BTU/LB	FT/S	V/S	COND	P/RAN	T	R			
360	1.0978-1	5.4890 0	-988.4	1.8810	1.7226	1.56492	1.4057	1.2950	0.2478	1.3845	926.6	0.286	.0092	.7730	360		
380	1.0400-1	5.2001 0	-983.4	1.8945	1.7360	1.5776	1.4191	1.3084	0.2480	1.3839	951.8	0.281	.0097	.7669	380		
400	9.8802-2	4.9401 0	-978.0	1.9072	1.7487	1.5903	1.4319	1.3211	0.2483	1.3833	976.4	0.316	.0103	.7649	400		
420	9.0982-2	4.7049 0	-973.5	1.9193	1.7609	1.6024	1.4440	1.3332	0.2486	1.3827	1000.2	0.331	.0108	.7615	420		
440	8.9820-2	4.4910 0	-968.5	1.9309	1.7724	1.6140	1.4555	1.3448	0.2489	1.3820	1023.5	0.345	.0113	.7586	440		
460	8.5915-2	4.2958 0	-963.5	1.9419	1.7835	1.6251	1.4666	1.3559	0.2493	1.3812	1046.2	0.359	.0118	.7562	460		
480	8.2335-2	4.1168 0	-958.5	1.9526	1.7941	1.6357	1.4772	1.3665	0.2497	1.3805	1068.4	0.373	.0123	.7543	480		
500	7.9042-2	3.9521 0	-953.6	1.9628	1.8043	1.6459	1.4874	1.3767	0.2501	1.3796	1090.1	0.386	.0128	.7528	500		
520	7.6002-2	3.8001 0	-948.5	1.9726	1.8141	1.6557	1.4973	1.3865	0.2505	1.3787	1111.4	0.400	.0133	.7517	520		
537	7.3641-2	3.6821 0	-944.4	1.9805	1.8221	1.6636	1.5052	1.3944	0.2509	1.3780	1128.7	0.411	.0137	.7510	537		
540	7.3187-2	3.6594 0	-943.5	1.9820	1.8236	1.6652	1.5067	1.3960	0.2509	1.3778	1132.2	0.413	.0138	.7509	540		
560	7.0573-2	3.5287 0	-938.5	1.9912	1.8327	1.6743	1.5159	1.4051	0.2514	1.3768	1152.5	0.426	.0143	.7508	560		
580	6.8140-2	3.4070 0	-933.5	2.0000	1.8416	1.6831	1.5247	1.4339	0.2519	1.3758	1172.1	0.439	.0147	.7509	580		
600	6.5868-2	3.2934 0	-928.4	2.0086	1.8501	1.6917	1.5332	1.4224	0.2524	1.3748	1192.1	0.452	.0152	.7511	600		
620	6.3743-2	3.1872 0	-923.4	2.0168	1.8584	1.7000	1.5415	1.4338	0.2529	1.3737	1211.3	0.464	.0156	.7513	620		
640	6.1752-2	3.0876 0	-918.3	2.0249	1.8664	1.7080	1.5496	1.4383	0.2535	1.3727	1230.2	0.476	.0161	.7511	640		
660	5.9880-2	2.9940 0	-913.2	2.0327	1.8742	1.7158	1.5574	1.4466	0.2540	1.3715	1248.8	0.489	.0165	.7506	660		
680	5.8119-2	2.9060 0	-908.2	2.0403	1.8818	1.7234	1.5650	1.4542	0.2546	1.3704	1267.0	0.501	.0170	.7500	680		
700	5.6459-2	2.8229 0	-903.1	2.0477	1.8892	1.7308	1.5723	1.4610	0.2552	1.3692	1285.0	0.513	.0175	.7493	700		
720	5.4890-2	2.7445 0	-897.9	2.0549	1.8964	1.7380	1.5795	1.4688	0.2558	1.3680	1302.7	0.524	.0179	.7487	720		
740	5.3407-2	2.6703 0	-892.8	2.0619	1.9034	1.7450	1.5866	1.4758	0.2564	1.3668	1320.0	0.536	.0184	.7483	740		
760	5.2001-2	2.6001 0	-887.7	2.0687	1.9103	1.7518	1.5934	1.4827	0.2571	1.3655	1337.1	0.547	.0188	.7481	760		
780	5.06668-2	2.5334 0	-882.5	2.0754	1.9170	1.7585	1.6001	1.4893	0.2577	1.3643	1354.0	0.558	.0192	.7479	780		
800	4.9401-2	2.4701 0	-877.4	2.0820	1.9235	1.7651	1.6066	1.4959	0.2584	1.3630	1370.6	0.569	.0197	.7478	800		
820	4.8196-2	2.4098 0	-872.2	2.0883	1.9299	1.7715	1.6130	1.5023	0.2590	1.3617	1387.0	0.580	.0201	.7477	820		
840	4.7049-2	2.3524 0	-867.0	2.0946	1.9361	1.7777	1.6193	1.5085	0.2597	1.3604	1403.1	0.591	.0205	.7477	840		
860	4.5955-2	2.2977 0	-861.8	2.1007	1.9423	1.7838	1.6254	1.5146	0.2604	1.3591	1419.1	0.602	.0210	.7477	860		
880	4.4910-2	2.2455 0	-856.6	2.1067	1.9483	1.7898	1.6314	1.5206	0.2611	1.3558	1434.8	0.613	.0214	.7477	880		
900	4.3912-2	2.1956 0	-851.4	2.1126	1.9541	1.7957	1.6372	1.5265	0.2618	1.3565	1450.3	0.623	.0218	.7478	900		
920	4.2958-2	2.1479 0	-846.1	2.1183	1.9599	1.8015	1.6430	1.5323	0.2626	1.3552	1465.6	0.634	.0223	.7476	920		
940	4.2044-2	2.1022 0	-840.9	2.1240	1.9656	1.8071	1.6487	1.5377	0.2633	1.3538	1480.7	0.644	.0227	.7474	940		
—	—	—	—	—	—	—	—	—	—	—	—	—	—	—	—	—	
960	4.1168-2	2.0584 0	-835.6	2.1295	1.9711	1.8127	1.6542	1.5435	0.2640	1.3525	1495.6	0.654	.0231	.7472	960		
980	4.0328-2	2.0164 0	-830.3	2.1350	1.9766	1.8181	1.6597	1.5489	0.2648	1.3511	1510.4	0.664	.0236	.7469	980		
1000	3.9521-2	1.9760 0	-825.0	2.1404	1.9819	1.8235	1.6650	1.5543	0.2655	1.3498	1524.9	0.675	.0240	.7466	1000		
1020	3.8746-2	1.9373 0	-819.7	2.1456	1.9872	1.8287	1.6703	1.5595	0.2663	1.3484	1539.3	0.685	.0244	.7463	1020		
1040	3.8001-2	1.9000 0	-814.4	2.1508	1.9924	1.8339	1.6755	1.5647	0.2671	1.3471	1553.6	0.695	.0249	.7460	1040		
—	—	—	—	—	—	—	—	—	—	—	—	—	—	—	—	—	
-1060	3.7228-2	1.8642 0	-809.0	2.1559	1.9975	1.8390	1.6806	1.5698	0.2678	1.3457	1567.7	0.704	.0253	.7457	1060		
-1080	3.6593-2	1.8297 0	-803.6	2.1609	2.0025	1.8490	1.6856	1.5748	0.2686	1.3444	1581.6	0.714	.0257	.7453	1080		
-1100	3.5928-2	1.7964 0	-798.3	2.1658	2.0074	1.8490	1.6905	1.5798	0.2694	1.3431	1595.4	0.724	.0262	.7449	1100		
-1120	3.5287-2	1.7643 0	-792.9	2.1707	2.0123	1.8538	1.6954	1.5846	0.2702	1.3417	1609.0	0.734	.0266	.7445	1120		
-1140	3.4668-2	1.7334 0	-787.5	2.1755	2.0171	1.8586	1.7002	1.5894	0.2709	1.3404	1622.5	0.743	.0271	.7440	1140		

TABLE 19A CONTINUED - PROPERTIES BASED ON CONSTANT GASEOUS COMPOSITIONS

FUEL H/C ATOM RATIO = 2.100; DRY AIR;		F/A=0.050248; EQUIV. RATIO= 0.750; GASEOUS COMPOSITION: CO ₂ = .09804; H ₂ O= .10262; N ₂ = .74077; MW = 28.8596;		CHEM. EQUIV. RATIO= 0.7504; H ₂ O= .04968; AR= .00888	
T	DENSITY (P=1.0) (P=50.0)	H	(P=.01) (P=1.0)	ENTROPY (P=1.0) (P=10.)	(P=50.)
R	LB/FT ³	LB/FT ³	BTU/LB	BTU/ LB R	BTU/ LB R
116.0	3.4070-2	1.7035 0	-782.0	2.1802	2.0218
118.0	3.3492-2	1.6746 0	-776.6	2.1849	2.0264
120.0	3.2934-2	1.6467 0	-771.1	2.1895	2.0310
122.0	3.2394-2	1.6197 0	-765.7	2.1940	2.0355
124.0	3.1872-2	1.5936 0	-760.2	2.1984	2.0400
126.0	3.1366-2	1.5683 0	-754.7	2.2028	2.0444
128.0	3.0876-2	1.5438 0	-749.1	2.2072	2.0487
130.0	3.0401-2	1.5200 0	-743.6	2.2115	2.0530
132.0	2.9940-2	1.4970 0	-738.0	2.2157	2.0573
134.0	2.9493-2	1.4747 0	-732.5	2.2199	2.0615
136.0	2.9060-2	1.4530 0	-726.9	2.2240	2.0656
138.0	2.8638-2	1.4319 0	-721.3	2.2281	2.0697
140.0	2.8229-2	1.4115 0	-715.7	2.2322	2.0737
142.0	2.7832-2	1.3916 0	-710.0	2.2362	2.0777
144.0	2.7445-2	1.3723 0	-704.4	2.2401	2.0817
146.0	2.7069-2	1.3535 0	-698.7	2.2440	2.0856
148.0	2.6703-2	1.3352 0	-693.1	2.2479	2.0894
150.0	2.6347-2	1.3174 0	-687.4	2.2517	2.0933
152.0	2.6001-2	1.3000 0	-681.0	2.2555	2.0970
154.0	2.5663-2	1.2831 0	-675.9	2.2592	2.1008
156.0	2.5334-2	1.2667 0	-670.2	2.2629	2.1045
158.0	2.5013-2	1.2507 0	-664.4	2.2666	2.1081
160.0	2.4701-2	1.2350 0	-658.7	2.2702	2.1118
162.0	2.4396-2	1.2198 0	-652.9	2.2738	2.1154
164.0	2.4098-2	1.2049 0	-647.1	2.2774	2.1189
166.0	2.3808-2	1.1904 0	-641.3	2.2809	2.1224
168.0	2.3524-2	1.1762 0	-635.5	2.2844	2.1259
170.0	2.3246-2	1.1624 0	-629.6	2.2878	2.1294
172.0	2.2977-2	1.1489 0	-623.8	2.2912	2.1328
174.0	2.2713-2	1.1357 0	-617.9	2.2946	2.1362
176.0	2.2455-2	1.1228 0	-612.0	2.2980	2.1395
178.0	2.2203-2	1.1101 0	-606.2	2.3013	2.1429
180.0	2.1956-2	1.0978 0	-600.3	2.3046	2.1462
190.0	2.0801-2	1.0600 0	-570.6	2.3207	2.1622
200.0	1.9760-2	9.8802-1	-540.6	2.3361	2.1776
210.0	1.8820-2	9.4098-1	-510.3	2.3508	2.1924
220.0	1.7964-2	8.9820-1	-479.8	2.3650	2.2066
-230.0	1.7183-2	8.5915-1	-449.0	2.3787	2.2202
2400	1.6467-2	8.2335-1	-418.0	2.3919	2.2334
2500	1.5808-2	7.9042-1	-386.8	2.4046	2.2462

TABLE 14A CONCLUDED . - PROPERTIES BASED ON CONSTANT GASEOUS COMPOSITIONS

FUEL H/C ATOM RATIO = 2.100; DRY AIR;		H (P=1.0)		ENTROPY (P=.10)		CP (P=1.0)		GAM (P=50.)		VIS FT/S		COND BTU/FT HR		PRAN R	
T	R	DENSITY (P=50.)	LB/FT ³	BTU/LB	BTU/LB R	BTU/LB	BTU/LB R	BTU/LB	BTU/LB R	BTU/LB	BTU/LB R	BTU/LB	BTU/LB R	BTU/LB	BTU/LB R
2600	1.5200-2	7.6002-1	-355.4	2.4170	2.2585	2.1001	1.9416	1.8309	0.3153	1.2791	2393.7	1316	0.0569	.7293	2600
2700	1.4637-2	7.3187-1	-323.7	2.9289	2.2705	2.1120	1.9536	1.8428	0.3173	1.2770	2437.2	1350	0.0587	.7289	2700
2800	1.4115-2	7.0573-1	-291.9	2.4405	2.2820	2.1236	1.9651	1.8544	0.3191	1.2750	2480.0	1383	0.0606	.7282	2800
2900	1.3628-2	6.8140-1	-259.9	2.4517	2.2933	2.1348	1.9764	1.8656	0.3208	1.2731	2522.0	1415	0.0624	.7275	2900
3000	1.3174-2	6.5868-1	-227.8	2.4626	2.3042	2.1457	1.9873	1.8765	0.3224	1.2713	2563.4	1448	0.0642	.7269	3000
3100	1.2749-2	6.3744-1	-195.4	2.4732	2.3147	2.1563	1.9979	1.8871	0.3239	1.2697	2604.1	1479	0.0660	.7262	3100
3200	1.2350-2	6.1752-1	-163.0	2.4835	2.3251	2.1666	2.0082	1.8974	0.3254	1.2682	2644.2	1511	0.0678	.7255	3200
3300	1.1976-2	5.9880-1	-130.4	2.4935	2.3351	2.1766	2.0182	1.9075	0.3267	1.2668	2683.7	1542	0.0695	.7248	3300
3400	1.1624-2	5.8119-1	-97.6	2.5033	2.3669	2.1864	2.0280	1.9172	0.3280	1.2655	2722.6	1573	0.0712	.7240	3400
3500	1.1292-2	5.6659-1	-64.8	2.5128	2.3544	2.1959	2.0375	1.9268	0.3292	1.2643	2761.1	1603	0.0729	.7233	3500
3600	1.0978-2	5.4890-1	-31.8	2.5221	2.3637	2.2052	2.0468	1.9360	0.3303	1.2631	2799.0	1633	0.0746	.7226	3600
3700	1.0681-2	5.3407-1	-3.3	2.5312	2.3727	2.2143	2.0559	1.9451	0.3314	1.2621	2836.4	1663	0.0763	.7220	3700
3800	1.0400-2	5.2001-1	34.5	2.5400	2.3816	2.2231	2.0647	1.9540	0.3324	1.2611	2873.3	1692	0.0780	.7214	3800
3900	1.0134-2	5.0668-1	67.8	2.5487	2.3918	2.2318	2.0734	1.9626	0.3333	1.2601	2909.8	1721	0.0796	.7208	3900
4000	9.8802-3	4.9401-1	101.1	2.5571	2.3987	2.2402	2.0818	1.9711	0.3342	1.2593	2945.8	1750	0.0812	.7202	4000
4100	9.6393-3	4.8196-1	134.6	2.5654	2.4069	2.2485	2.0901	1.9793	0.3350	1.2585	2981.5	1778	0.0828	.7195	4100
4200	9.4098-3	4.7049-1	168.1	2.5735	2.4150	2.2566	2.0981	1.9874	0.3358	1.2577	3016.7	1807	0.0844	.7189	4200
4300	9.1909-3	4.5955-1	201.8	2.5814	2.4229	2.2645	2.1061	1.9953	0.3366	1.2570	3051.5	1834	0.0860	.7182	4300
4400	8.9820-3	4.4910-1	235.5	2.5891	2.4307	2.2722	2.1138	2.0031	0.3373	1.2563	3086.1	1870	0.0875	.7175	4400
4500	8.7824-3	4.3912-1	269.2	2.5967	2.4383	2.2798	2.1214	2.0106	0.3380	1.2557	3120.1	1890	0.0891	.7168	4500
4600	8.5915-3	4.2958-1	303.0	2.6042	2.4457	2.2873	2.1288	2.0181	0.3386	1.2551	3153.8	1917	0.0906	.7160	4600
4700	8.4087-3	4.2044-1	336.9	2.6114	2.4530	2.2946	2.1361	2.0254	0.3392	1.2545	3187.2	1944	0.0922	.7151	4700
4800	8.2335-3	4.1168-1	370.9	2.6186	2.4601	2.3017	2.1433	2.0325	0.3398	1.2540	3220.2	1970	0.0937	.7143	4800
4900	8.0655-3	4.0328-1	404.9	2.6256	2.4672	2.3087	2.1503	2.0395	0.3403	1.2535	3252.9	2023	0.0953	.7134	4900
5000	7.9042-3	3.9521-1	438.9	2.6325	2.4740	2.3156	2.1572	2.0464	0.3408	1.2530	3285.3	2023	0.0968	.7126	5000
5100	7.7492-3	3.8746-1	473.0	2.6392	2.4808	2.3224	2.1639	2.0532	0.3413	1.2525	3317.4	2049	0.0983	.7119	5100
5200	7.6002-3	3.8001-1	507.2	2.6459	2.4874	2.3290	2.1705	2.0598	0.3418	1.2521	3349.1	2075	0.0998	.7111	5200
5300	7.4568-3	3.7284-1	541.4	2.6524	2.4939	2.3355	2.1771	2.0663	0.3423	1.2516	3380.6	2101	0.1012	.7104	5300
5400	7.3187-3	3.6594-1	575.7	2.6588	2.5003	2.3419	2.1835	2.0727	0.3427	1.2512	3411.8	2126	0.1027	.7096	5400

